PHYSICAL REVIEW D **91,** 085020 (2015)

Symmetry improvement of 3PI effective actions for O(N) scalar field theory

Michael J. Brown* and Ian B. Whittingham

College of Science, Technology and Engineering, James Cook University, Townsville 4811, Australia

(Received 12 February 2015; published 14 April 2015)

N-particle irreducible effective actions (nPIEA) are a powerful tool for extracting nonperturbative and nonequilibrium physics from quantum field theories. Unfortunately, practical truncations of nPIEA can unphysically violate symmetries. Pilaftsis and Teresi (PT) addressed this by introducing a "symmetry improvement" scheme in the context of the 2PIEA for an O (2) scalar theory, ensuring that the Goldstone boson is massless in the broken symmetry phase [A. Pilaftsis and D. Teresi, Nucl. Phys. B874, 594 (2013)]. We extend this idea by introducing a symmetry improved 3PIEA for O(N) theories, for which the basic variables are the one-, two- and three-point correlation functions. This requires the imposition of a Ward identity involving the three-point function. We find that the method leads to an infinity of physically distinct schemes, though a field theoretic analogue of d'Alembert's principle is used to single out a unique scheme. The standard equivalence hierarchy of nPIEA no longer holds with symmetry improvement, and we investigate the difference between the symmetry improved 3PIEA and 2PIEA. We present renormalized equations of motion and counterterms for two- and three-loop truncations of the effective action, though we leave their numerical solution to future work. We solve the Hartree-Fock approximation and find that our method achieves a middle ground between the unimproved 2PIEA and PT methods. The phase transition predicted by our method is weakly first order and the Goldstone theorem is satisfied, while the PT method correctly predicts a second-order phase transition. In contrast, the unimproved 2PIEA predicts a strong first-order transition with large violations of the Goldstone theorem. We also show that, in contrast to PT, the two-loop truncation of the symmetry improved 3PIEA does not predict the correct Higgs decay rate, although the three-loop truncation does, at least to leading order. These results suggest that symmetry improvement should not be applied to nPIEA truncated to $< n$ loops. We also show that symmetry improvement schemes are compatible with the Coleman-Mermin-Wagner theorem, giving a check on the consistency of the formalism.

DOI: 10.1103/PhysRevD.91.085020 PACS numbers: 11.15.Tk, 05.10.-a, 11.30.−j

I. INTRODUCTION

The recent demands of nonequilibrium field theory applications in particle physics, cosmology and condensed matter have led to a renaissance in the development of novel field theory methods. The S-matrix school, rebooted in the guise of spinor-helicity methods, has led to a dramatic speedup in the computation of gauge theory scattering amplitudes in vacuum [1]. On the finite temperature and density fronts, efficient functional methods in the form of n-particle irreducible effective actions (nPIEA) have proven useful to understand collective behavior and phase transitions [2]. They are similar in spirit to methods based on Schwinger-Dyson equations in field theory or Bogoliubov-Born-Green-Kirkwood-Yvon (BBGKY) equations in kinetic theory; however, unlike the Schwinger-Dyson or BBGKY equations, nPIEA naturally form closed systems of equations of motion without requiring any closure ansatz [3–5]. nPIEA methods can be understood as a hybrid of variational and perturbative methods: nPIEA consist of a series of Feynman diagrams; however, the propagators and vertices of these diagrams are the *exact* 1- through n-point proper connected correlation functions which are determined self-consistently using variational equations of motion.

This self-consistency effectively resums certain classes of perturbative Feynman diagrams to infinite order. For example, the one-loop 2PIEA diagram corresponding to the Hartree-Fock self-energy in ϕ^4 theory actually sums all of the so-called daisy and super-daisy graphs of ordinary perturbation theory (Fig. 1). This particular resummation is often done in the literature without the use of nPIEA, but such *ad hoc* resummation schemes run the risk of summing an asymptotic series: a mathematically dangerous operation (recent progress on summability has been made in *resurgence* theory [6], which is beyond the scope of this work). nPIEA sidestep this issue because they are defined by the rigorous Legendre transform procedure, guaranteeing equivalence with the original theory. Unlike *ad hoc* resummations, nPIEA based approximation schemes are placed on a firm theoretical footing and can be systematically improved.

However, loop-wise truncations of nPIEA, $n > 1$, have difficulties in the treatment of theories with spontaneously broken continuous symmetries. The root cause of these difficulties is the fact that nPIEA obey different Ward

*michael.brown6@my.jcu.edu.au

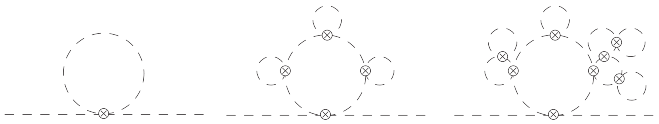

FIG. 1. From left to right: the Hartree-Fock self-energy diagram, an example daisy or ring diagram, an example super-daisy graph. The whole class of super-daisy diagrams is obtained from iterating insertions of Hartree-Fock graphs in all possible ways.

identities than the 1PIEA. When the effective action is truncated to a finite order the equivalence between the Ward identities is lost. This can also be understood in terms of the resummation of perturbative Feynman diagrams: when an nPIEA is truncated some subset of perturbative diagrams are summed to infinite order, but the complementary subset is left out entirely. The pattern of resummations does not guarantee that the cancellations between perturbative diagrams needed to maintain the symmetry are kept. In the case of scalar field theories with $\mathrm{O}(N) \to \mathrm{O}(N-1)$ breaking, the result is that the final $\mathrm{O}(N-1)$ symmetry is maintained, but, at the Hartree-Fock level of approximation, the nonlinearly realized $\mathrm{O}(N)/\mathrm{O}(N-1)$ is lost, the Goldstone theorem is violated (the $N-1$ Goldstone bosons are massive), and the symmetry restoration phase transition is first order in contradiction with the second-order transition expected on the basis of universality arguments. A similar problem arises in gauge theories, where the violation of gauge invariance in the l-loop truncation is due to the missing $(l+1)$-loop diagrams (see, e.g. [7,8] for a discussion of the gauge fixing problem).

Several studies have attempted to find a remedy for this problem. These are discussed in [9] and references therein. Here we restrict attention to the technique most frequently advocated in the literature [10]. This technique constructs the so-called *external propagator* as the second functional derivative of a resummed effective action which depends only on the mean field, obtained by eliminating the 2- through n-point correlation functions of the nPIEA by their equations of motion. The resulting effective action does obey a 1PI type Ward identity and the external propagator yields massless Goldstone bosons. However, the external propagator is not the propagator used in loop graphs, so the loop corrections still contain massive Goldstone bosons leading to incorrect thresholds, decay rates and violations of unitarity. In order to avoid these problems a manifestly self-consistent scheme must be used.

Pilaftsis and Teresi recently developed a method which circumvents these difficulties [9] for the widely used 2PIEA (also known as the CJT effective action after Cornwall, Jackiw and Tomboulis [11], the Luttinger-Ward functional or Φ-derivable approximation depending on the context). The idea is incredibly simple: impose the desired Ward identities directly on the free correlation functions. This is consistently implemented by using Lagrange multipliers. The remarkable point is that the resulting equations of motion can be put into a form that completely eliminates the Lagrange multiplier field. They achieve this by taking a limit in which the Lagrange multiplier vanishes from all but one of the equations of motion, and this remaining equation of motion is replaced with the constraint to obtain a closed system. We show that this nontrivial aspect of the procedure generalizes to the 3PIEA. We find that the generalization requires a careful consideration of the variational procedure, however, and an infinity of schemes are possible. A new principle is required to choose between the schemes, and we propose what we call the *d'Alembert formalism* as the appropriate principle by analogy to the constrained variational problem in mechanics.

We extend the work of Pilaftsis and Teresi to the 3PIEA for three reasons. First, the 3PIEA is known to be the required starting point to obtain a self-consistent non-equilibrium kinetic theory of gauge theories. The accurate calculation of transport coefficients and thermalization times in gauge theories requires the use of nPIEA with $n \geq 3$ (see, e.g. [2,10,12] and references therein for discussion). The fundamental reason for this is that the 3PIEA includes medium induced effects on the three-point vertex at leading order. The 2PIEA in gauge theory contains a dressed propagator but not a dressed vertex, leading not only to an inconsistency of the resulting kinetic equation but also to a spurious gauge dependence of the kind discussed previously. We consider this work to be a stepping stone towards a fully self-consistent, nonperturbative and manifestly gauge invariant treatment of out-of-equilibrium gauge theories.

Second, nPIEA allows one to accurately describe the initial value problem with 1- to n-point connected correlation functions in the initial state. For example, the widely used 2PIEA allows one to solve the initial value problem for initial states with a Gaussian density matrix. However, the physical applications one has in mind typically start from a near thermal equilibrium state which is not well approximated by a Gaussian density matrix. This leads to problems with renormalization, unphysical transient responses and thermalization to the wrong temperature [13]. This is addressed in [13] by the addition of an infinite set of nonlocal vertices which only have support at the initial time. Going to $n > 2$ allows one to better describe the initial state, thereby reducing the need for additional nonlocal vertices.

Lastly, the infinite hierarchy of nPIEA is the natural home for the widely used 2PIEA (in all its guises) and provides the clearest route for systematic improvements over existing treatments. Thus investigating symmetry improvement of 3PIEA is a well-motivated next step in the development of nonperturbative quantum field theory.

After this introductory section we review nPIEA in Sec. II, focusing on the 3PIEA for a model $\mathrm{O}(N)$ scalar

field theory with symmetry breaking as a specific example. Then in Sec. III we review and extend the symmetry improvement program of Pilaftsis and Teresi. This includes a derivation of the required Ward identities, their implementation as constraints using Lagrange multipliers and the limiting procedure required to obtain sensible equations of motion for the system. We will see that this procedure rests on a certain technical assumption which we will justify in Appendix A and make a connection to the d'Alembert principle using a mechanical analogy. Then in Sec. IV we investigate the renormalization of the theory, first with the two-loop truncation and then three loops. The three-loop truncation is analytically intractable in $1+3$ dimensions so, after discussing the renormalization procedure in arbitrary dimension, we present results for $1+2$ dimensions. The result of this section is a set of finite equations of motion which must be solved numerically. In Sec. V we solve the theory at the Hartree-Fock level and discuss the phase transition thermodynamics. Section VI is a verification that the Coleman-Mermin-Wagner theorem holds in the symmetry improvement formalism despite the imposition of Ward identities, a check on the consistency of the formalism. In Sec. VII we discuss the effects of symmetry improvement on the absorptive parts of propagators and make some comments involving the Higgs decay rate and dispersion relations. Finally in Sec. VIII we discuss the main themes of the paper and point out directions for future work.

On notation: we work mostly in $1+3$ dimensions with $\eta_{\mu\nu}=\mathrm{diag}(1,-1,-1,-1)$, although the generalization to other dimensions is simple. We take $\hbar=c=k_{\mathrm{B}}=1$ as far as units are concerned, though we keep loop counting factors of $\hbar$ explicit. Repeated indices are summed. Often, field indices accompany spacetime arguments. Repeated indices in this case imply an integration over the corresponding spacetime argument as well ("DeWitt notation"). Where explicitly indicated, spacetime and momentum integrals are written in compressed notation with $\int_x \equiv \int \mathrm{d}^4x$, $\int_p \equiv \int \mathrm{d}^4p/(2\pi)^4$ and $\int_{\boldsymbol{p}} \equiv \int_{\boldsymbol{p}} \mathrm{d}^3\boldsymbol{p}/(2\pi)^3$ etc. $\langle \mathrm{T}[\cdots]\rangle$ represents the time-ordered product of the factors in $[\cdots]$. Through most of this article the meaning of time ordering is left implicit. The formalism can be readily applied to vacuum field theory ($t\in(-\infty,+\infty)$ with the natural ordering), finite temperature field theory in the imaginary time or Matsubara formalism ($t\to -i\tau$, with periodic boundary conditions on $\tau\in[0,\beta=\frac{1}{k_{\mathrm{B}}T})$ and the natural ordering on τ) [14], and general nonequilibrium field theory on the two-time Schwinger-Keldysh contour (t runs from 0 to $+\infty$ then from $+\infty-i\epsilon$ back down to $0-i\epsilon$ with time ordering in the sense of position along the contour rather than the magnitude $|t|$) [15]. In Sec. IV we develop the renormalization theory for the vacuum case and in Sec. V we solve the Hartree-Fock approximation at finite temperature in the Matsubara formalism.

II. REVIEW OF nPI EFFECTIVE ACTIONS

For the sake of having an explicit example, we consider the $\mathrm{O}(N)$ linear σ model given by the action

$$S[\phi]=\int_x \frac{1}{2}\partial_\mu\phi_a\partial^\mu\phi^a-\frac{1}{2}m^2\phi_a\phi^a-\frac{\lambda}{4!}(\phi_a\phi^a)^2, \tag{2.1}$$

where $a=1,\ldots,N$ is the flavor index. In the symmetry breaking regime $m^2<0$ and a vacuum expectation value develops, which by symmetry can be taken in the last component $\langle\phi\rangle=(0,\ldots,0,v)$ where $v^2=-6m^2/\lambda$ at tree level. The massive mode, which we loosely call "the Higgs" [reflecting our ultimate interest in the Standard Model, despite the absence of gauge interactions in (2.1)], gets a tree-level mass $m_H^2=\lambda v^2/3=-2m^2$.

The nPI effective actions form a systematic hierarchy of functionals $\Gamma^{(n)}[\varphi,\Delta,V,\ldots,V^{(n)}]$ where $\varphi,\ldots,V^{(n)}$ are the proper 1- through n-point correlation functions and we have suppressed spacetime arguments and flavor indices. In more detail,

$$\varphi_a=\langle\phi_a\rangle, \tag{2.2}$$

$$\Delta_{ab}=i\hbar(\langle \mathrm{T}[\phi_a\phi_b]\rangle-\langle\phi_a\rangle\langle\phi_b\rangle), \tag{2.3}$$

$$\begin{aligned}\hbar^2\Delta_{ad}\Delta_{be}\Delta_{cf}V_{def}=&\langle \mathrm{T}[\phi_a\phi_b\phi_c]\rangle-\langle \mathrm{T}[\phi_a\phi_b]\rangle\langle\phi_c\rangle\\&-\langle \mathrm{T}[\phi_c\phi_a]\rangle\langle\phi_b\rangle-\langle \mathrm{T}[\phi_b\phi_c]\rangle\langle\phi_a\rangle\\&+2\langle\phi_a\rangle\langle\phi_b\rangle\langle\phi_c\rangle\\&\vdots\end{aligned} \tag{2.4}$$

In general $V^{(n)}$ is the sum of connected one particle irreducible Feynman diagrams contributing to $\langle\phi^n\rangle$ with all external legs (including leg corrections) removed.

In the absence of external source terms the correlation functions obey equations of motion of the form

$$\frac{\delta\Gamma^{(n)}}{\delta\varphi}=0,\frac{\delta\Gamma^{(n)}}{\delta\Delta}=0,\ldots,\frac{\delta\Gamma^{(n)}}{\delta V^{(n)}}=0. \tag{2.5}$$

In the exact theory $\Gamma^{(n)}$ obey equivalence relationships

$$\Gamma^{(1)}[\varphi]=\Gamma^{(2)}[\varphi,\Delta]=\Gamma^{(3)}[\varphi,\Delta,V]=\ldots, \tag{2.6}$$

where extra arguments are eliminated by their equations of motion when comparisons are made. These relationships only hold approximately when approximations are made to the theory. A stronger equivalence hierarchy that relates loop-wise truncations of the $\Gamma^{(n)}$ will be discussed below.

For later convenience we introduce the tree-level vertex functions

$$V_{0abc}(x,y,z) = \left.\frac{\delta^3 S[\phi]}{\delta\phi_a(x)\delta\phi_b(y)\delta\phi_c(z)}\right|_{\phi=\varphi}, \quad (2.7)$$

$$W_{abcd}(x,y,z,w) = \left.\frac{\delta^4 S[\phi]}{\delta\phi_a(x)\delta\phi_b(y)\delta\phi_c(z)\delta\phi_d(w)}\right|_{\phi=\varphi}. \quad (2.8)$$

For the O(N) model these are

$$V_{0abc}(x,y,z) = -\frac{\lambda}{3}[\delta_{ab}\varphi_c(x) + \delta_{ca}\varphi_b(x) + \delta_{bc}\varphi_a(x)] \times \delta^{(4)}(x-y)\delta^{(4)}(x-z), \quad (2.9)$$

$$W_{abcd}(x,y,z,w) = -\frac{\lambda}{3}[\delta_{ab}\delta_{cd} + \delta_{ac}\delta_{bd} + \delta_{ad}\delta_{bc}] \times \delta^{(4)}(x-y)\delta^{(4)}(x-z)\delta^{(4)}(x-w). \quad (2.10)$$

The nPIEA is defined in the functional integral formalism by the Legendre transform of the connected generating function

$$W^{(n)}[J, K^{(2)}, \cdots, K^{(n)}] = -i\hbar \ln Z^{(n)}[J, K^{(2)}, \cdots, K^{(n)}], \quad (2.11)$$

for a field theory in the presence of source terms defined by the generating functional

$$Z^{(n)}[J, K^{(2)}, \ldots, K^{(n)}] = \int \mathcal{D}[\phi] \exp\frac{i}{\hbar}\left(S[\phi] + J_x\phi_x + \frac{1}{2}\phi_x K^{(2)}_{xy}\phi_y + \cdots + \frac{1}{n!}K^{(n)}_{x_1\cdots x_n}\phi_{x_1}\cdots\phi_{x_n}\right). \quad (2.12)$$

Then $\Gamma^{(n)}$ is the n-fold Legendre transform

$$\Gamma^{(n)}[\varphi, \Delta, V, \ldots, V^{(n)}] = W^{(n)} - J\frac{\delta W^{(n)}}{\delta J} - K^{(2)}\frac{\delta W^{(n)}}{\delta K^{(2)}} - \cdots - K^{(n)}\frac{\delta W^{(n)}}{\delta K^{(n)}}, \quad (2.13)$$

where the source terms $J, K^{(2)}, \ldots, K^{(n)}$ are solved for in terms of the $\varphi, \Delta, \ldots, V^{(n)}$. Spacetime integrations and O(N) index contractions have been suppressed for brevity. For bosonic fields the $\Delta, \ldots, V^{(n)}$ are totally symmetric under permutations of their arguments. The generalization to fermions requires sign changes for odd permutations of arguments corresponding to fermionic fields, but is otherwise straightforward. (Note that the nPIEA is defined by this Legendre transform, *not* by any irreducibility property of the Feynman graphs, though for low enough loop orders the graphs are irreducible as the name implies. At high enough loop order for $n > 2$ the name becomes misleading. For example, the five-loop 5PIEA contains graphs that are not five-particle irreducible [4]!)

$\Gamma^{(1)}[\varphi]$ is the familiar 1PI effective action introduced by Goldstone, Salam and Weinberg and independently by Jona-Lasinio [16]. $\Gamma^{(1)}[\varphi]$ can be written

$$\Gamma^{(1)}[\varphi] = S[\varphi] + \frac{i\hbar}{2}\mathrm{Tr}\ln\{\Delta_0^{-1}[\varphi]\} + \Gamma_2^{(1)}[\varphi], \quad (2.14)$$

where $\Delta_0^{-1}[\varphi] = \delta^2 S[\phi+\varphi]/\delta\phi^2|_{\phi=0}$ is the inverse propagator and $\Gamma_2^{(1)}$ is the sum of all connected vacuum graphs with ≥ 2 loops where the propagators $\Delta_0[\varphi]$ and vertices are obtained from the shifted action $S[\phi+\varphi]$ with the additional prescription that all 1-particle reducible graphs are dropped [17]. Note that (2.4) is equivalent to

$$V^{(1)}_{def}(u,v,w) = \frac{\delta^3\Gamma^{(1)}}{\delta\varphi_d(u)\delta\varphi_e(v)\delta\varphi_f(w)}, \quad (2.15)$$

where the superscript "(1)" indicates the vertex derived from the 1PIEA.

The 2PIEA $\Gamma^{(2)}[\varphi, \Delta]$ was introduced in the context of nonrelativistic statistical mechanics, apparently independently, by Lee and Yang, Luttinger and Ward, and others, but was brought to the functional formalism and relativistic field theory by Cornwall, Jackiw and Tomboulis [11]. $\Gamma^{(2)}[\varphi, \Delta]$ is most easily computed by noting that the Legendre transform can be performed in stages. First perform the Legendre transform with respect to J, using result (2.14) with the replacement $S[\phi] \to S[\phi] + \frac{1}{2}\phi_x K^{(2)}_{xy}\phi_y$, then do the transform with respect to $K^{(2)}$. This procedure leads to (up to an irrelevant constant)

$$\Gamma^{(2)}[\varphi, \Delta] = S[\varphi] + \frac{i\hbar}{2}\mathrm{Tr}\ln(\Delta^{-1}) + \frac{i\hbar}{2}\mathrm{Tr}(\Delta_0^{-1}\Delta) + \Gamma_2^{(2)}[\varphi, \Delta]. \quad (2.16)$$

The equation of motion for Δ is Dyson's equation,

$$\Delta^{-1} = \Delta_0^{-1} - \Sigma, \quad (2.17)$$

where

$$\Sigma = \frac{2i}{\hbar}\frac{\delta\Gamma_2^{(2)}[\varphi,\Delta]}{\delta\Delta}, \tag{2.18}$$

is identified as the 1PI self-energy. Since Σ consists of 1PI two-point graphs, $\Gamma_2^{(2)}$ must consist of 2PI vacuum graphs. That is, $\Gamma_2^{(2)}$ is the sum of all vacuum diagrams which do not fall apart when any two lines are cut. This results in a drastic reduction in the number of graphs at a given loop order. Further, the propagators in a 2PI graph are the full propagators Δ, with all self-energy insertions resummed to infinite order.

The 3PIEA $\Gamma^{(3)}[\varphi,\Delta,V]$ can be computed following the same method: replace $S[\phi] \to S[\phi] + \frac{1}{3!}K^{(3)}_{xyz}\phi_x\phi_y\phi_z$ in the previous result and perform the Legendre transform with respect to $K^{(3)}$.

The shift by the source term $K^{(3)}$ results in the introduction of an effective three-point vertex $\tilde{V} \equiv V_0 + K^{(3)}$ appearing in $\Gamma_2^{(2)}$. The difficult step of the Legendre transform is relating $\tilde{V}$ to V. This can be done by comparing $\delta W^{(3)}[J,K^{(2)},K^{(3)}]/\delta K^{(3)}$ with $\delta\Gamma^{(2)}[\varphi,\Delta;\tilde{V}]/\delta K^{(3)}$ (see [2,18]). The final result for $\Gamma^{(3)}$ is

$$\Gamma^{(3)} = S[\varphi] + \frac{i\hbar}{2}\mathrm{Tr}\ln(\Delta^{-1}) + \frac{i\hbar}{2}\mathrm{Tr}(\Delta_0^{-1}\Delta) + \Gamma_3^{(3)}, \tag{2.19}$$

where to three-loop order the diagram piece is

$$\Gamma_3^{(3)} = \Phi_1 + \frac{\hbar^2}{3!}V_0\Delta\Delta\Delta V - \Phi_2 + \Phi_3 + \Phi_4 + \Phi_5 + \mathcal{O}(\hbar^4), \tag{2.20}$$

where $\Phi_1,\ldots,\Phi_5$ are given by the Feynman diagrams shown in Fig. 2. Explicitly,

$$\Phi_1 = -\frac{\hbar^2}{8}W_{abcd}\Delta_{ab}\Delta_{cd}, \tag{2.21}$$

$$\Phi_2 = \frac{\hbar^2}{12}V_{abc}V_{def}\Delta_{ad}\Delta_{be}\Delta_{cf}, \tag{2.22}$$

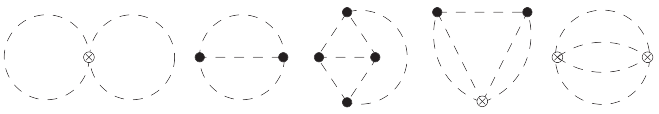

FIG. 2. Two- and three-loop diagrams contributing to $\Gamma_3^{(3)}[\varphi,\Delta,V]$. We label these Φ_1 through Φ_5 from left to right, respectively, and their explicit forms are given in (2.21) through (2.25). Solid circles represent the resummed vertices V and the crossed circles represent the bare vertices V_0 and W. The dashed lines represent the resummed propagators Δ. Note that these diagrams are called "EIGHT," "EGG," "MERCEDES," "HAIR," and "BBALL," respectively, in the nomenclature of [4,5].

$$\Phi_3 = \frac{i\hbar^3}{4!}V_{abc}V_{def}V_{ghi}V_{jkl}\Delta_{ad}\Delta_{bg}\Delta_{cj}\Delta_{eh}\Delta_{fk}\Delta_{il}, \tag{2.23}$$

$$\Phi_4 = -\frac{i\hbar^3}{8}V_{abc}V_{def}W_{ghij}\Delta_{ad}\Delta_{bg}\Delta_{ch}\Delta_{ei}\Delta_{fj}, \tag{2.24}$$

$$\Phi_5 = \frac{i\hbar^3}{48}W_{abcd}W_{efgh}\Delta_{ae}\Delta_{bf}\Delta_{cg}\Delta_{dh}. \tag{2.25}$$

The 3PI equation of motion for V is $0 = \frac{\delta\Gamma^{(3)}}{\delta V_{abc}}$, which reads in full

$$V_{abc} = V_{0abc} + i\hbar V_{ade}V_{bfg}V_{chi}\Delta_{df}\Delta_{eh}\Delta_{gi} - \frac{1}{3!}\sum_\pi \frac{3i\hbar}{2}V_{\pi(a)de}W_{\pi(b)\pi(c)fg}\Delta_{df}\Delta_{eg} + \mathcal{O}(\hbar^2), \tag{2.26}$$

where $\sum_\pi$ is a sum over the 3! permutations mapping $(a,b,c) \to (\pi(a),\pi(b),\pi(c))$ (spacetime arguments are permuted as well). The graphical interpretation of this equation is shown in Fig. 3. The permutations lead to the usual s, t, and u channel contributions with the expected symmetry factors. This equation is best thought of as a self-consistent integral equation in the same spirit as a Schwinger-Dyson equation, and can be solved iteratively. By iterating (2.26) one sees that it sums a sequence of vertex correction diagrams to infinite order.

If all higher-order terms are kept in $\Gamma_3^{(3)}$, the resulting V is the same as the $V^{(1)}$ of (2.15); however, truncated actions give solutions $V \neq V^{(1)}$. Similar remarks apply for the propagators. These self-consistent solutions do not, in general, obey the desirable field theoretic properties of the full solution, such as Ward identities. The symmetry improvement strategy is to impose 1PI Ward identities as constraints on the self-consistent solutions Δ and V. This is discussed further in Sec. III.

Note that (2.26) can be derived by removing a resummed vertex from each graph in $\Gamma_3^{(3)}$ (because $\delta/\delta V$ acts by removing a single V factor from graphs in all possible ways), which has the graphical effect of opening two loops. This means that the one-loop correction to V comes from three-loop graphs in $\Gamma^{(3)}$. Thus a loop-wise truncation of nPIEA for $n \geq 3$ does not lead to a loop-wise truncation of

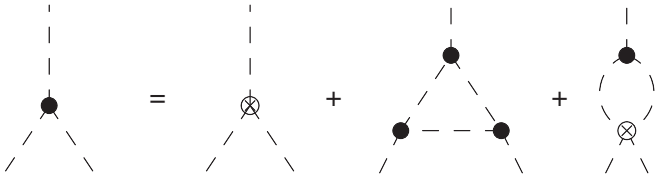

FIG. 3. Equation of motion for the 3PI vertex function V up to one-loop order (2.26). Note that the bubble graph (last term) is implicitly symmetrized over external momenta and O(N) indices.

the corresponding equations of motion. We will discuss the further implications of this in Sec. VII.

Another important implication of this result is that $\Gamma^{(2)}$ and $\Gamma^{(3)}$ are equivalent to two-loop order (after one substitutes $V = V_0 + \mathcal{O}(\hbar)$ in $\Gamma^{(3)}$). However, $\Gamma^{(2)}$ and $\Gamma^{(3)}$ differ at three-loop order because $\Gamma^{(3)}$ contains resummed vertex corrections that $\Gamma^{(2)}$ does not. This is an example of an equivalence hierarchy of nPI effective actions that has the general form [2]:

$$\Gamma^{(1)}_{(1\,\mathrm{loop})}[\phi] = \Gamma^{(2)}_{(1\,\mathrm{loop})}[\phi,\Delta] = \cdots, \tag{2.27}$$

$$\Gamma^{(1)}_{(2\,\mathrm{loop})}[\phi] \neq \Gamma^{(2)}_{(2\,\mathrm{loop})}[\phi,\Delta] = \Gamma^{(3)}_{(2\,\mathrm{loop})}[\phi,\Delta,V] = \cdots, \tag{2.28}$$

$$\begin{aligned}\Gamma^{(1)}_{(3\,\mathrm{loop})}[\phi] &\neq \Gamma^{(2)}_{(3\,\mathrm{loop})}[\phi,\Delta] \neq \Gamma^{(3)}_{(3\,\mathrm{loop})}[\phi,\Delta,V] \\ &= \Gamma^{(4)}_{(3\,\mathrm{loop})}[\phi,\Delta,V,V^{(4)}] = \cdots, \\ &\vdots\end{aligned} \tag{2.29}$$

where the subscripts represent the order of the loop-wise truncation and the "extra" correlation functions are to be evaluated at the solutions of their respective equations of motion before making the comparison (and also allowance is made for shifts by irrelevant constants). This equivalence hierarchy has been explicitly checked up to five-loop 5PI order in scalar field theories [4].

The existence of the equivalence hierarchy implies that in the standard formalism one gains nothing by going to higher nPI effective actions unless one also includes diagrams with at least n loops, since for $m > n$ one can always reduce $\Gamma^{(m)}_{(n\mathrm{loop})}$ to $\Gamma^{(n)}_{(n\mathrm{loop})}$. However, we shall see that symmetry improvement breaks this equivalence hierarchy. In particular, we find that the symmetry improvement of the 3PI effective action modifies the Δ equation of motion in a way that remains nontrivial even if $\Gamma^{(3)}$ is then truncated at two loops and V is replaced by its tree-level value V_0. In general we find that the symmetry improvement procedure introduces Ward identities that relate k-point functions to $(k+1)$-point functions and these constraints spoil the equivalence hierarchy; i.e. the "operations" of symmetry improvement and reduction in the hierarchy do not commute. The consequences of this for the phase diagram of the scalar $\mathrm{O}(N)$ theory in the various possible schemes are investigated in Sec. V.

III. SYMMETRY IMPROVEMENT

Symmetry improvement begins with the consideration of the Ward identities in the nPI formalism. Following [9] we derive the Ward identities from the condition that the effective action is invariant under a symmetry transformation. The theory in (2.1) has the $\mathrm{O}(N)$ symmetry transform

$$\phi_a \to \phi_a + i\epsilon_A T^A_{ab}\phi_b, \tag{3.1}$$

where T^A are the generators of the group in the fundamental representation ($A = 1,\ldots,N(N-1)/2$) and ϵ_A are infinitesimal transformation parameters. Note that our implicit integration convention can be maintained if we consider that T^A_{ab} contains a spacetime delta function $T^A_{ab} \propto \delta^{(4)}(x_a - x_b)$. Also $T^A_{ab} = -T^A_{ba}$. Under this transformation the effective actions change by

$$\delta\Gamma^{(1)} = \frac{\delta\Gamma^{(1)}}{\delta\varphi_a} i\epsilon_A T^A_{ab}\varphi_b, \tag{3.2}$$

$$\delta\Gamma^{(2)} = \frac{\delta\Gamma^{(2)}}{\delta\varphi_a} i\epsilon_A T^A_{ab}\varphi_b + \frac{\delta\Gamma^{(2)}}{\delta\Delta_{ab}} i\epsilon_A (T^A_{ac}\Delta_{cb} + T^A_{bc}\Delta_{ac}), \tag{3.3}$$

$$\begin{aligned}\delta\Gamma^{(3)} =& \frac{\delta\Gamma^{(3)}}{\delta\varphi_a} i\epsilon_A T^A_{ab}\varphi_b + \frac{\delta\Gamma^{(3)}}{\delta\Delta_{ab}} i\epsilon_A (T^A_{ac}\Delta_{cb} + T^A_{bc}\Delta_{ac}) \\ &+ \frac{\delta\Gamma^{(3)}}{\delta V_{abc}} i\epsilon_A (T^A_{ad}V_{dbc} + T^A_{bd}V_{adc} + T^A_{cd}V_{abd}), \\ &\vdots\end{aligned} \tag{3.4}$$

according to the tensorial structure of the arguments. The next steps to derive the Ward identities are to set $\delta\Gamma^{(n)} = 0$, take functional derivatives of the resulting equations with respect to φ and finally apply the equations of motion. We also extract the overall factors of $i\epsilon_A$. We call the identity derived from the mth derivative of $\delta\Gamma^{(n)}$ the $(m+1)$-point nPI Ward identity, denoted by $\mathcal{W}^{A(n)}_{a_1\ldots a_m} = 0$ where $a_1,\ldots,a_m$ are $\mathrm{O}(N)$/spacetime indices. We note first of all that $\mathcal{W}^{(n)} = 0$ identically by the equations of motion. We also find that

$$\mathcal{W}^{A(1)}_c = \frac{\delta\Gamma^{(1)}}{\delta\varphi_c\delta\varphi_a} T^A_{ab}\varphi_b, \tag{3.5}$$

$$\mathcal{W}^{A(1)}_{cd} = \frac{\delta\Gamma^{(1)}}{\delta\varphi_d\delta\varphi_c\delta\varphi_a} T^A_{ab}\varphi_b + \frac{\delta\Gamma^{(1)}}{\delta\varphi_c\delta\varphi_a} T^A_{ad} + \frac{\delta\Gamma^{(1)}}{\delta\varphi_d\delta\varphi_a} T^A_{ac}. \tag{3.6}$$

Specializing now to the broken symmetry vacuum $\varphi_b = v\delta_{bN}$, we obtain the following identities by substituting different generators T^A_{ab} in turn:

$$0 = \int_{x_a} \Delta^{-1}_{ca}(x_c,x_a)v, \qquad a \neq N, \tag{3.7}$$

$$\begin{aligned}0 =& \int_z V_{Nab}(x,y,z)v + \Delta^{-1}_{ab}(x,y) \\ &- \delta_{ab}\Delta^{-1}_{NN}(x,y), \qquad a,b \neq N\end{aligned} \tag{3.8}$$

$$0 = \Delta^{-1}_{ca}, \qquad a \neq c, \tag{3.9}$$

$$0 = \int_z V_{dca}(x,y,z)v, \qquad d,c,a \neq N, \tag{3.10}$$

$$0 = \int_z V_{NNa}(x,y,z)v, \qquad a \neq N. \tag{3.11}$$

Note that we explicitly write spacetime arguments, $O(N)$ indices and integrations in the above. This is because DeWitt notation would lead to ambiguities here. Below we introduce an ansatz adapted to the situation which again allows for notational simplifications.

The essence of symmetry improvement is to impose these Ward identities, derived for the 1PI correlation functions, on the nPI correlation functions. Effectively, we change $f(\Delta_{1\mathrm{PI}}, V_{1\mathrm{PI}}) \to f(\Delta_{3\mathrm{PI}}, V_{3\mathrm{PI}})$, where f is the Ward identity and we change the arguments but not the functional form. We have already made this substitution in (3.7)–(3.11).

The first two identities will prove important in the following, however, the identities (3.9)–(3.11) are trivial in the sense that they can be satisfied simply by postulating an ansatz for Δ and V which is tensorial under the unbroken $\mathrm{O}(N-1)$ symmetry. For later convenience we adopt this spontaneous symmetry breaking (SSB) ansatz now by introducing the notation

$$\Delta_{ab}(x,y) = \begin{cases} \Delta_G(x,y), & a = b \neq N, \\ \Delta_H(x,y), & a = b = N, \\ 0, & \text{otherwise}, \end{cases} \tag{3.12}$$

for the Goldstone (Δ_G) and Higgs (Δ_H) propagators, respectively, and we also introduce the vertex functions $\bar{V}$ and V_N where

$$V_{abc}(x,y,z) = \begin{cases} \bar{V}(x,y,z)\delta_{aN}\delta_{bc} & \text{exactly one of} \\ \quad +\text{cyclic permutations} & a,b,c = N, \\ V_N(x,y,z) & a = b = c = N, \\ 0 & \text{otherwise}. \end{cases} \tag{3.13}$$

Note that V_N is not constrained by any of the 2- or 3-point Ward identities. Spacetime arguments are permuted along with the $\mathrm{O}(N)$ indices, so that the first spacetime argument of $\bar{V}$ is always the one referring to the Higgs. The other two arguments refer to the Goldstone bosons and $\bar{V}$ is symmetric under their interchange. V_N is totally symmetric in its arguments. For reference note that at the two-loop truncation, $V = V_0$ and we obtain $\bar{V} = (-\lambda v/3) \times \delta^{(4)}(x-y)\delta^{(4)}(x-z)$ and $V_N = 3\bar{V}$. After substituting the ansatz the diagrams $\Phi_1, \ldots, \Phi_5$ can be put into the form

$$\Phi_1 = \frac{\hbar^2\lambda}{24}(N^2-1)\Delta_G\Delta_G + \frac{\hbar^2\lambda}{12}(N-1)\Delta_G\Delta_H + \frac{\hbar^2\lambda}{8}\Delta_H\Delta_H, \tag{3.14}$$

$$\Phi_2 = \frac{\hbar^2}{4}(N-1)\bar{V}\,\bar{V}\,\Delta_H\Delta_G\Delta_G + \frac{\hbar^2}{12}V_N V_N(\Delta_H)^3, \tag{3.15}$$

$$\Phi_3 = (N-1)\frac{i\hbar^3}{3!}V_N(\bar{V})^3(\Delta_H)^3(\Delta_G)^3 + \frac{i\hbar^3}{4!}(V_N)^4(\Delta_H)^6 + (N-1)\frac{i\hbar^3}{8}(\bar{V})^4\Delta_H\Delta_H(\Delta_G)^4, \tag{3.16}$$

$$\Phi_4 = \frac{i\hbar^3\lambda}{24}[2(N-1)\bar{V}V_N(\Delta_H)^3\Delta_G\Delta_G + (N^2-1)\bar{V}\,\bar{V}\,\Delta_H(\Delta_G)^4 + 3V_N V_N(\Delta_H)^5 + 2^2(N-1)\bar{V}\,\bar{V}\,(\Delta_G)^3\Delta_H\Delta_H], \tag{3.17}$$

$$\Phi_5 = \frac{i\hbar^3\lambda^2}{144}\{[(N-1)\Delta_G\Delta_G + \Delta_H\Delta_H]^2 + 2(N-1)(\Delta_G)^4 + 2(\Delta_H)^4\}. \tag{3.18}$$

The suppressed spacetime integrations can be restored by comparing these expressions to the diagrams and using the fact that $\bar{V}$ vertices join one Higgs and two Goldstone lines, while V_N vertices join three Higgs lines. (These expressions can be checked using the supplemental MATHEMATICA notebook [19].)

In terms of the SSB ansatz variables the nontrivial Ward identities are $O(N)$-scalar equations which read

$$0 = \mathcal{W}_1 \equiv \int_z \Delta_G^{-1}(x,z)v, \tag{3.19}$$

$$0 = \mathcal{W}_2 \equiv \int_z \bar{V}(x,y,z)v + \Delta_G^{-1}(x,y) - \Delta_H^{-1}(x,y). \tag{3.20}$$

The physical meaning of these can be seen by assuming translation invariance, substituting

$$\Delta_{G/H}^{-1}(p) \equiv \int_{x-y} \mathrm{e}^{ip\cdot(x-y)}\Delta_{G/H}^{-1}(x,y) = p^2 - m_{G/H}^2 - \Sigma_{G/H}(p), \tag{3.21}$$

and $\bar{V} = (-\lambda v/3) \times \delta^{(4)}(x-y)\delta^{(4)}(x-z) + \delta\bar{V}$ where $\delta\bar{V}$ represents the loop corrections to the vertex. Matching powers of $\hbar$ (which are implicit in $\Sigma_{G/H}$ and $\delta\bar{V}$) results in

$$vm_G^2 = 0, \tag{3.22}$$

$$-\frac{\lambda v^2}{3} + m_H^2 - m_G^2 = 0, \tag{3.23}$$

$$\delta\bar{V}(p,-p,0)v + \Sigma_H(p) - \Sigma_G(p) = 0, \tag{3.24}$$

which are Goldstone's theorem, the tree-level relation between the particle masses, and a relation between the vertex correction (with one external Goldstone boson leg set to zero momentum) and the self-energies of the Higgs and Goldstone bosons, respectively. The imaginary part of this last identity can be used to extract a relation between the Higgs decay rate and the off-shell Goldstone boson self-energy and vertex corrections. This will be investigated in Sec. VII.

We now wish to impose (3.19)–(3.20) as constraints on the allowable values of φ, Δ and V in the 3PIEA. First we review the 2PIEA case as discussed in [9], which imposes (3.19) on $\Gamma^{(2)}$ through the introduction of Lagrange multiplier fields $\ell_A^d(x)$, where A is an O(N) adjoint index, and the symmetry improved effective action which we write in manifestly covariant form as

$$\tilde{\Gamma}[\varphi,\Delta,\ell] = \Gamma^{(2)}[\varphi,\Delta] + \frac{i}{2}\int_x \ell_A^d(x)\mathcal{W}_c^{A(1)}(x)[P_T(\varphi,x)]_{cd}. \tag{3.25}$$

The transverse projector,

$$[P_T(\varphi,x)]_{cd} = \delta_{cd} - \frac{\varphi_c(x)\varphi_d(x)}{\varphi^2(x)}, \tag{3.26}$$

ensures that only the Goldstone modes are involved in the constraint. The equations of motion follow from $\delta\tilde{\Gamma}/\delta\varphi = \delta\tilde{\Gamma}/\delta\Delta = 0$.

Substituting the SSB ansatz and using translation invariance gives

$$\tilde{\Gamma}[\varphi,\Delta,\ell] = \Gamma^{(2)}[\varphi,\Delta] - \ell\mathcal{W}_1, \tag{3.27}$$

where we have absorbed group theory factors in ℓ. The 2PI equations of motion become

$$\frac{\partial\Gamma^{(2)}/VT}{\partial v} = \ell\frac{\partial}{\partial v}\mathcal{W}_1, \tag{3.28}$$

$$\frac{\delta\Gamma^{(2)}}{\delta\Delta_G(x,y)} = -v\ell\left[\int_x \Delta_G^{-1}(x,0)\right]^2, \tag{3.29}$$

$$\frac{\delta\Gamma^{(2)}}{\delta\Delta_H(x,y)} = 0, \tag{3.30}$$

$$0 = v\int_y \Delta_G^{-1}(x,y). \tag{3.31}$$

The factor of VT on the left-hand side of the first equation is the volume of spacetime, which we have divided by to give an intensive quantity.

Now applying the constraint with $v \neq 0$ directly in the equations of motion would give zero right-hand sides, reducing to the standard 2PI formalism. This is valid in the full theory because the Ward identity is satisfied. However, this is impossible in the case where the 2PI effective action is truncated at finite loop order because the actual Ward identity obeyed by the 2PIEA is $\mathcal{W}_c^{A(2)} \neq \mathcal{W}_c^{A(1)}$. The manifestation of this fact in the symmetry improvement formalism is a singularity: $\ell \to \infty$ as $v\int\Delta_G^{-1} \to 0$ so as to leave a finite right-hand side in the first equation of motion.

It is now necessary to introduce the constraint through a limit process, and choose the scaling of ℓ in the limit such that the scalar equation of motion is traded for the constraint. To this end we set

$$v\int_y \Delta_G^{-1}(x,y) = \eta m^3, \tag{3.32}$$

and take the limit $\eta \to 0$. Note that, in extension of Pilaftsis and Teresi [9], one may allow separate regulators η_i for each Goldstone mode $i = 1,\ldots,N-1$, but there is nothing much to gain from this and it leads to no new difficulties so we take a common regulator $\eta_i = \eta$. m is an arbitrary fixed mass scale, conveniently taken to be $\sim m_H$, which serves to make η dimensionless. The modified equations of motion become

$$\frac{\partial\Gamma^{(2)}/VT}{\partial v} = \frac{\ell\eta}{v}m^3, \tag{3.33}$$

$$\frac{\delta\Gamma^{(2)}}{\delta\Delta_G(z,w)} = -\frac{\ell\eta^2}{v}m^6. \tag{3.34}$$

If we choose to scale η and the ℓ such that $\ell_0 \equiv \ell\eta/v$ is a constant and $\ell\eta^2/v \to 0$ then

$$\frac{\partial\Gamma^{(2)}/VT}{\partial v} = \ell_0 m^3, \tag{3.35}$$

$$\frac{\delta\Gamma^{(2)}}{\delta\Delta_G(z,w)} = 0, \tag{3.36}$$

in addition to the Ward identity and the Δ_H equation of motion. In practice, in the symmetry broken phase, one

simply discards the first equation of motion and solves the second one in conjunction with the Ward identity, which suffices to give a closed system. In the symmetric phase $v = 0$ and the Ward identity is trivial, but $\Gamma^{(2)}$ also does not depend linearly on v, hence one can take the previous equations of motion with $\ell_0 = 0$. Note that we can, and do, keep a nonzero m_G^2 in the intermediate stages of the computation to serve as an infrared regulator.

To recap the procedure: first we define a symmetry improved effective action using Lagrange multipliers and compute the equations of motion. Second, note that the equations of motion are singular when the constraints are applied. Third, regulate the singularity by slightly violating the constraint. Fourth, pass to a suitable limit where violation of the constraint tends to zero. We require the limiting procedure to be universal in the sense that no additional data (arbitrary forms of the Lagrange multiplier fields) need be introduced into the theory.

We now extend this logic to the 3PI case. To that end we introduce the symmetry improved 3PIEA

$$\tilde{\Gamma}^{(3)} = \Gamma^{(3)} + \frac{i}{2}\int_x \ell_A^d(x)\mathcal{W}_c^{A(1)}(x)[P_T(\varphi,x)]_{cd} - Bf[\mathcal{W}_{cd}^{A(1)}], \tag{3.37}$$

where the second term is the same as the 2PI symmetry improvement term and the third term contains the extended symmetry improvement. B is the new Lagrange multiplier and $f[\mathcal{W}_{cd}^{A(1)}]$ is an arbitrary functional which vanishes if and only if its argument vanishes. Substituting the SSB ansatz we obtain

$$\tilde{\Gamma}^{(3)} = \Gamma^{(3)} - \ell\mathcal{W}_1 - Bf[\mathcal{W}_2]. \tag{3.38}$$

The equations of motion are

$$\frac{\partial\Gamma^{(3)}/VT}{\partial v} = \ell_0 m^3 + B\int_{xz}\frac{\delta f}{\delta\mathcal{W}_2(x,y)}\bar{V}(x,y,z), \tag{3.39}$$

$$\frac{\delta\Gamma^{(3)}}{\delta\Delta_G(r,s)} = -B\int_{xy}\frac{\delta f}{\delta\mathcal{W}_2(x,y)}\Delta_G^{-1}(x,r)\Delta_G^{-1}(s,y), \tag{3.40}$$

$$\frac{\delta\Gamma^{(3)}}{\delta\Delta_H(r,s)} = B\int_{xy}\frac{\delta f}{\delta\mathcal{W}_2(x,y)}\Delta_H^{-1}(x,r)\Delta_H^{-1}(s,y), \tag{3.41}$$

$$\frac{\delta\Gamma^{(3)}}{\delta\bar{V}(r,s,t)} = vB\int_{xyz}\frac{\delta f}{\delta\mathcal{W}_2(x,y)} \times\delta^{(4)}(x-r)\delta^{(4)}(y-s)\delta^{(4)}(z-t), \tag{3.42}$$

$$\frac{\delta\Gamma^{(3)}}{\delta V_N(r,s,t)} = 0, \tag{3.43}$$

$$\mathcal{W}_1 = 0, \tag{3.44}$$

$$\mathcal{W}_2 = 0, \tag{3.45}$$

where we already take the previous limiting procedure to eliminate ℓ and $\mathcal{W}_1$. In (3.42) we have inserted a factor of $1 = \int_z \delta^{(4)}(z-t)$ for later convenience. Now we devise a limiting procedure such that the right-hand sides of two of (3.40), (3.41) and (3.42) vanish. The remaining equation must be chosen so that it can be replaced by the constraint (3.45) and still give a closed system. Note that (3.42) cannot be eliminated because there is not enough information to reconstruct $\bar{V}$ from $\Delta_{G/H}$ using $\mathcal{W}_2$. Thus we must eliminate either Δ_G or Δ_H, or else artificially restrict the form of $\bar{V}$.

We show that the desired simplification of the equations of motion can be achieved without restricting $\bar{V}$ under the assumption that $\delta f/\delta\mathcal{W}_2(x,y)$ is a spacetime independent constant. Note that this is not required by Poincaré invariance (only the weaker condition $\delta f/\delta\mathcal{W}_2(x,y) = g(|x-y|^2)$ is mandated). We temporarily adopt this assumption without further explanation, though in Appendix A we will show that it can be justified by the introduction of the *d'Alembert formalism*.

Computing the left-hand side of (3.42) using (2.19) and displaying only the two-loop terms explicitly we obtain

$$\frac{\delta\Gamma^{(3)}}{\delta\bar{V}(r,s,t)} = -\frac{\hbar^2}{2}(N-1) \times\int_{xyz}\left(\bar{V}(x,y,z) + \frac{\lambda v}{3}\delta(x-y)\delta(x-z)\right) \times\Delta_H(x,r)\Delta_G(y,s)\Delta_G(z,t) + \mathcal{O}(\hbar^3). \tag{3.46}$$

Without symmetry improvement one sets this quantity to zero, giving an equation equivalent to the one we derived in the previous section, (2.26) (up to a group theory factor, since the variables in the one case are Δ_{ab} and V and in the other Δ_G, Δ_H and $\bar{V}$). This equation is now modified by the symmetry improvement to

$$-\frac{\hbar^2}{2}(N-1)\int_{xyz}\left(\bar{V}(x,y,z) + \frac{\lambda v}{3}\delta(x-y)\delta(x-z)\right) \times\Delta_H(x,r)\Delta_G(y,s)\Delta_G(z,t) + \mathcal{O}(\hbar^3) = vB\int_{xyz}\frac{\delta f}{\delta\mathcal{W}_2(x,y)}\delta^{(4)}(x-r)\delta^{(4)}(y-s)\delta^{(4)}(z-t). \tag{3.47}$$

Convolving with the inverse propagators $\Delta_H^{-1}\Delta_G^{-1}\Delta_G^{-1}$ gives

$$-\frac{\hbar^2}{2}(N-1)\left(\bar{V}(a,b,c)+\frac{\lambda v}{3}\delta(a-b)\delta(a-c)\right)+\mathcal{O}(\hbar^3)$$
$$=vB\int_{xyz}\frac{\delta f}{\delta\mathcal{W}_2(x,y)}\Delta_H^{-1}(x,a)\Delta_G^{-1}(y,b)\Delta_G^{-1}(z,c)$$
$$=\left[B\int_{xy}\frac{\delta f}{\delta\mathcal{W}_2(x,y)}\Delta_H^{-1}(x,a)\Delta_G^{-1}(y,b)\right]\mathcal{W}_1. \quad (3.48)$$

The right-hand side now vanishes due to (3.44). With the regulator (3.32) in place, we have that the symmetry improvement term in the $\bar{V}$ equation of motion vanishes faster than the naive $B\delta f/\delta\mathcal{W}_2$ scaling manifest in (3.42). Schematically, the right-hand side scales as $B(\delta f/\delta\mathcal{W}_2)m_H^2m_G^4v\sim B(\delta f/\delta\mathcal{W}_2)m_H^8\eta^2/v$. So long as $B\delta f/\delta\mathcal{W}_2$ does not blow up as fast as η^{-2} as $\eta\to 0$ the symmetry improvement has no effect on $\bar{V}$.

Now we investigate the Goldstone propagator. Substituting (2.19) into (3.40) we find the symmetry improved equation of motion for Δ_G,

$$\Delta_G^{-1}(r,s)=\Delta_{0G}^{-1}(r,s)-\tilde{\Sigma}_G(r,s), \quad (3.49)$$

where we have defined the 3PI symmetry improved self-energy,

$$\tilde{\Sigma}_G(r,s)\equiv\frac{2i}{\hbar(N-1)}\left[\frac{\delta\Gamma_3}{\delta\Delta_G(r,s)}+B\int_{xy}\frac{\delta f}{\delta\mathcal{W}_2(x,y)}\Delta_G^{-1}(x,r)\Delta_G^{-1}(s,y)\right]. \quad (3.50)$$

Substituting in $\Gamma_3^{(3)}$ to two-loop order, we find

$$\tilde{\Sigma}_G(r,s)$$
$$=\frac{i\hbar\lambda}{6}\mathrm{Tr}[(N+1)\Delta_G+\Delta_H]\delta^{(4)}(r-s)$$
$$-i\hbar\int_{abcd}\left(\bar{V}(a,b,r)+\frac{2\lambda v}{3}\delta^{(4)}(a-r)\delta^{(4)}(b-r)\right)\times\bar{V}(c,d,s)\Delta_H(a,c)\Delta_G(b,d)$$
$$+\frac{2i}{\hbar(N-1)}B\int_{xy}\frac{\delta f}{\delta\mathcal{W}_2(x,y)}\Delta_G^{-1}(x,r)\Delta_G^{-1}(s,y)$$
$$+\mathcal{O}(\hbar^2). \quad (3.51)$$

The first term corresponds to the Hartree-Fock diagram (Fig. 1, far left); the second term corresponds to the sunset diagrams (Fig. 4) and the third term is the symmetry improvement term. The equation of motion for Δ_H can be written in the same form with a suitable definition for a symmetry improved self energy $\tilde{\Sigma}_H(r,s)$, where the symmetry improvement term now has the form $\sim B\int(\delta f/\delta\mathcal{W}_2)\Delta_H^{-1}\Delta_H^{-1}$.

FIG. 4. Sunset self-energy graph.

If we assume $\delta f/\delta\mathcal{W}_2$ is constant, we find that $\tilde{\Sigma}_G$ and $\tilde{\Sigma}_H$ scale as $(B\delta f/\delta\mathcal{W}_2)m_G^4\sim(B\delta f/\delta\mathcal{W}_2)m_H^6\eta^2/v^2$ and $(B\delta f/\delta\mathcal{W}_2)m_H^4\sim(B\delta f/\delta\mathcal{W}_2)m_H^4\eta^0$, respectively. Thus, by choosing a regulator such that $B\delta f/\delta\mathcal{W}_2$ goes to a finite limit, the equations of motion for $\bar{V}$ and Δ_G are unmodified and the equation of motion for Δ_H is modified by a finite term. This is the desired limiting procedure. Adopting it gives the final set of equations of motion:

$$\frac{\delta\Gamma^{(3)}}{\delta\Delta_G(r,s)}=0, \quad (3.52)$$

$$\frac{\delta\Gamma^{(3)}}{\delta\bar{V}(r,s,t)}=0, \quad (3.53)$$

$$\frac{\delta\Gamma^{(3)}}{\delta V_N(r,s,t)}=0, \quad (3.54)$$

$$\mathcal{W}_1=0, \quad (3.55)$$

$$\mathcal{W}_2=0. \quad (3.56)$$

IV. RENORMALIZATION

Here we undertake a general description of the renormalization problem at zero temperature. Our detailed considerations follow in Secs. IV A and IV B for two- and three-loop truncations, respectively. Finite temperature results are given for the Hartree-Fock approximation in Sec. V. The two-loop renormalization of the theory in Sec. IV A is nontrivial already even though the vertex equation of motion can be solved trivially. This is because the symmetry improvement breaks the nPIEA equivalence hierarchy by modifying the Higgs equation of motion.

Generically, modifications of the equations of motion following from the 2PIEA will lead to an inconsistency of the renormalization procedure since the 2PIEA is self-consistently complete at two-loop order (in the action, i.e. one- loop order in the equations of motion). However, we will see that the wave function and propagator renormalization constants (normally trivial in ϕ^4 at one loop) provide the extra freedom required to obtain consistency. Then in Sec. IV B we will renormalize the theory at three loops. Nonperturbative counterterm calculations are generally much more difficult than the analogous perturbative calculations, hence many of the manipulations were performed in a supplemental Mathematica notebook [19]. The results of this section are finite equations of motion for renormalized quantities which must be solved numerically.

We leave the numerical implementation to future work, except in the case of the Hartree-Fock approximation.

We wish to demonstrate the renormalizability of the equations of motion (3.52)–(3.56). First we examine the symmetric phase, since on physical grounds SSB is irrelevant to renormalizability. In the symmetric phase $v = 0$ and the Ward identity (3.55) is trivially satisfied, while (3.56) requires $\Delta_G = \Delta_H$ as expected. Further, iteration shows that (3.53) and (3.54) have the solution $\bar{V} = V_N = 0$ as expected on general grounds: there is no three-point vertex in the symmetric phase. As a result, the symmetry improved 3PIEA in the symmetric phase is equivalent to the ordinary 2PIEA,

$$\tilde{\Gamma}^{(3)}[\varphi = 0, \Delta, V = 0] = \Gamma^{(2)}[\varphi = 0, \Delta], \tag{4.1}$$

which is known to be renormalizable, either by an implicit construction involving Bethe-Salpeter integral equations or an explicit algebraic BPHZ (Bogoliubov-Parasiuk-Hepp-Zimmerman) style construction which has nontrivial consistency requirements (but which has been shown to be equivalent to the Bethe-Salpeter method) [10,20,21]. Thus, only divergences arising from nonzero V pose any new conceptual problems.

We will extend the BPHZ style procedure of [20,22], which was adapted to symmetry improved 2PIEA by [9] and to 3PIEA for three dimensional pure glue QCD (without symmetry improvement) by [8]. The essence of the procedure is quite simple. Consider for example the quadratically divergent integral $\int_q i\Delta_{G/H}(q)$. Since $\Delta_{G/H}(q)$ is determined self-consistently this is a complicated integral which must be evaluated numerically. However, the UV behavior of the propagator should approach q^{-2} as $q \to \infty$. (Note that Weinberg's theorem [23] implies that the self-consistent propagators have this form up to powers of logarithms [22], though renormalization group theory shows the true large-momentum behavior of the propagators is a power law with an anomalous dimension. This implies that a truncated nPIEA does not effect a resummation of large logarithms.) Now we can add and subtract an integral with the same UV asymptotics,

$$\int_q i\Delta_{G/H}(q) = \int_q \left[i\Delta_{G/H}(q) - \frac{i}{q^2 - \mu^2 + i\epsilon} \right] + \int_q \frac{i}{q^2 - \mu^2 + i\epsilon}, \tag{4.2}$$

where μ is an arbitrary mass subtraction scale (not a cutoff scale). The first term is now only logarithmically divergent and the second term can be evaluated analytically in a chosen regularization scheme such as dimensional regularization. A further subtraction of this kind can render the first term finite.

We write the renormalized propagators as

$$\Delta^{-1}_{G/H} = p^2 - m^2_{G/H} - \Sigma_{G/H}(p), \tag{4.3}$$

$$\Sigma_{G/H}(p) = \Sigma^a_{G/H}(p) + \Sigma^0_{G/H}(p) + \Sigma^r_{G/H}(p), \tag{4.4}$$

where $m_{G/H}$ is the physical mass and the (renormalized) self-energies have been separated into pieces according to their asymptotic behavior: $\Sigma^a_{G/H}(p) \sim p^2(\ln p)^{c_1}$, $\Sigma^0_{G/H} \sim (\ln p)^{c_2}$ and $\Sigma^r_{G/H} \sim p^{-2}$ as $p \to \infty$, respectively. The pole condition requires $\Sigma_{G/H}(p^2 = m^2_{G/H}) = 0$. We also introduce the auxiliary propagator $\Delta^\mu_{G/H} = (p^2 - \mu^2 - \Sigma^a_{G/H}(p))^{-1}$. The propagator $\Delta_{G/H}$ can be expanded in $\Delta^\mu_{G/H}$:

$$\Delta_{G/H}(p) = \Delta^\mu_{G/H}(p) + [\Delta^\mu_{G/H}(p)]^2(m^2_{G/H} - \mu^2 + \Sigma^0_{G/H} + \Sigma^r_{G/H}) + \mathcal{O}([\Delta^\mu_{G/H}(p)]^3[\Sigma^0_{G/H}(p)]^2). \tag{4.5}$$

This allows us to extract the leading-order asymptotics of diagrams as $p \to \infty$.

We now do a similar analysis to isolate the leading asymptotics for V at large momentum. Suppressing $O(N)$ indices we can write $V(p_1, p_2, p_3) = \lambda v f(\frac{p_1}{v}, \frac{p_2}{v}, \frac{p_3}{v})$ where $p_1 + p_2 + p_3 = 0$. Now $V \to 0$ as $v \to 0$ implies that $f(\chi_1, \chi_2, \chi_3) \sim \chi^\alpha (\ln \chi)^{c_3}$, where $\alpha < 1$ and χ is representative of the largest scale among χ_1, χ_2 and χ_3. Now consider the vertex equation of motion (2.26) or Fig. 3. The triangle graph goes like $\int_\ell \ell^{3\alpha-6}(\ln \ell)^{3c_3-3c_1} \sim \chi^{3\alpha-2}(\ln \chi)^{3c_3-3c_1}$ if $\alpha \neq 2/3$ or $(\ln \chi)^{1+3c_3-3c_1}$ if $\alpha = 2/3$, which is dominated by the bubble graph which goes like $\int_\ell \ell^{\alpha-4}(\ln \ell)^{c_3-2c_1} \sim \chi^\alpha (\ln \chi)^{c_3-2c_1}$ if $\alpha \neq 0$ or $(\ln \chi)^{1+c_3-2c_1}$ if $\alpha = 0$. Thus, to a leading approximation the large momentum behavior is obtained by dropping the triangle graph from the equation of motion. This can also be seen by taking $v \to 0$ at fixed p_i which suppresses the triangle graph relative to the bubble graph.

We now define auxiliary vertex functions $\bar{V}^\mu$ and V^μ_N which have the same asymptotic behavior as $\bar{V}$ and V_N, respectively, though depend only on the auxiliary propagators. We define $\bar{V}^\mu$ and V^μ_N by taking the equations of motion for $\bar{V}$ and V_N, dropping the triangle graphs, and making the replacements $\bar{V} \to \bar{V}^\mu$, $V_N \to V^\mu_N$, and $\Delta_{G/H} \to \Delta^\mu_{G/H}$. These equations are shown in Fig. 5. This gives a pair of coupled linear integral equations, analogous to the Bethe-Salpeter equations, for $\bar{V}^\mu$ and V^μ_N which can be solved explicitly by iteration. (Details of this calculation are presented in Sec. IV B). Unfortunately the result is only analytically tractable in fewer than $1 + 3$ dimensions, so we confine the analytical results depending

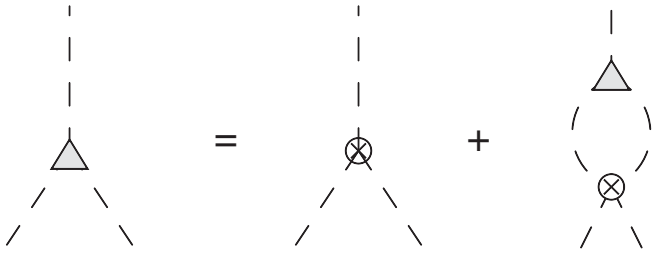

FIG. 5. Defining equation for the auxiliary vertex functions $\bar{V}^\mu$ and V_N^μ, obtained by taking the corresponding equations of motion for $\bar{V}$ and V_N, dropping the triangle graphs, and making the replacements $\bar{V} \to \bar{V}^\mu$, $V_N \to V_N^\mu$, and $\Delta_{G/H} \to \Delta_{G/H}^\mu$. The filled triangle represents the auxiliary vertices and the lines represent the auxiliary propagators. Crossed circles are bare vertices as before.

on the explicit forms of $\bar{V}^\mu$ and V_N^μ to this case. In the physically most interesting case of $1+3$ dimensions, $\bar{V}^\mu$ and V_N^μ must be numerically determined at the same time as $\bar{V}$ and V_N.

By using these auxiliary propagators and vertices we can isolate the divergent contributions to the equations of motion and so obtain the required set of counterterms to remove them.

A. Two-loop truncation

The theory simplifies dramatically at two-loop order. It follows from (2.26) that at this order $V \to V_0$ (up to a renormalization). Substituting this into the action gives, apart from the symmetry improvement terms, the standard 2PIEA. This is an example of the equivalence hierarchy previously discussed. Another simplification is that the logarithmic enhancement of the propagators in the UV due to $\Sigma_{G/H}^a$ vanishes at this level ($\Sigma_{G/H}^a$ is generated by the diagram Φ_5 appearing at three-loop order). In this case $\Delta_G^\mu = \Delta_H^\mu \equiv \Delta^\mu = (p^2 - \mu^2)^{-1}$. However, the reduction is not trivial because now the Higgs equation of motion has been replaced by a Ward identity. The equations of motion reduce to

$$\begin{aligned}\Delta_G^{-1}(x,y) = &-\left(\partial_\mu\partial^\mu + m^2 + \frac{\lambda}{6}v^2\right)\delta^{(4)}(x-y)\\ &-\frac{i\hbar}{6}(N+1)\lambda\Delta_G(x,x)\delta^{(4)}(x-y)\\ &-\frac{i\hbar}{6}\lambda\Delta_H(x,x)\delta^{(4)}(x-y)\\ &-\frac{i\hbar}{9}\lambda^2 v^2\Delta_H(x,y)\Delta_G(x,y),\end{aligned} \tag{4.6}$$

$$\Delta_H^{-1}(x,y) = -\frac{\lambda v^2}{3}\delta^{(4)}(x-y) + \Delta_G^{-1}(x,y), \tag{4.7}$$

$$v m_G^2 = 0. \tag{4.8}$$

The first line is the tree-level term, the second and third lines are the Hartree-Fock self-energies, the fourth line is the sunset self-energy, and the last two lines are the Ward identities $\mathcal{W}_2$ and $\mathcal{W}_1$, respectively.

To renormalize the theory we regard all parameters heretofore as bare parameters and introduce renormalized counterparts using the same letters:

$$(\phi, \varphi, v) \to Z^{1/2}(\phi, \varphi, v), \tag{4.9}$$

$$m^2 \to Z^{-1}Z_\Delta^{-1}(m^2 + \delta m^2), \tag{4.10}$$

$$\lambda \to Z^{-2}(\lambda + \delta\lambda), \tag{4.11}$$

$$\Delta \to Z Z_\Delta \Delta, \tag{4.12}$$

$$V \to Z^{-3/2} Z_V V. \tag{4.13}$$

Hereafter whenever we refer to a bare parameter we indicate this with a subscript "B," e.g. m_B^2 etc. The wave function renormalizations for Δ and V can be obtained from their definitions $\Delta \sim \langle\phi\phi\rangle$ and $\Delta\Delta\Delta V \sim \langle\phi\phi\phi\rangle$, respectively. Due to the presence of composite operators in the effective action, additional counterterms are required compared to the standard perturbation theory: δm_0^2 and $\delta\lambda_0$ for terms in the bare action, δm_1^2 for one-loop terms, $\delta\lambda_1^A$ for terms of the form $\phi_i\phi_i\Delta_{jj}$, $\delta\lambda_1^B$ for $\phi_i\phi_j\Delta_{ij}$ terms, $\delta\lambda_2^A$ for $\Delta_{ii}\Delta_{jj}$ and $\delta\lambda_2^B$ for $\Delta_{ij}\Delta_{ij}$. Similarly, Δ and V are given independent renormalization constants Z_Δ and Z_V, respectively. We give terms in the sunset graphs a universal $\delta\lambda$ counterterm.

The renormalized equations of motion are (see Appendix B for more detail)

$$\begin{aligned}\Delta_G^{-1}(p) = &\, Z Z_\Delta p^2 - m^2 - \delta m_1^2 - Z_\Delta\frac{\lambda + \delta\lambda_1^A}{6}v^2\\ &-\frac{\hbar}{6}[(N+1)\lambda + (N-1)\delta\lambda_2^A + 2\delta\lambda_2^B]Z_\Delta^2\mathcal{T}_G\\ &-\frac{\hbar}{6}(\lambda + \delta\lambda_2^A)Z_\Delta^2\mathcal{T}_H\\ &+ i\hbar\left[\frac{(\lambda+\delta\lambda)v}{3}\right]^2 Z_\Delta^3\mathcal{I}_{HG}(p),\end{aligned} \tag{4.14}$$

$$\Delta_H^{-1}(p) = -Z_\Delta\frac{(\lambda+\delta\lambda)v^2}{3} + \Delta_G^{-1}(p), \tag{4.15}$$

$$v m_G^2 = 0, \tag{4.16}$$

where for convenience we have defined

$$\mathcal{T}_{G/H} = \int_q i\Delta_{G/H}(q), \tag{4.17}$$

$$\mathcal{I}_{HG}(p) = \int_q i\Delta_H(q) i\Delta_G(p-q). \tag{4.18}$$

The tadpole integrals $\mathcal{T}_{G/H}$ correspond to the Hartree-Fock graphs and $\mathcal{I}_{HG}(p)$ corresponds to the sunset self-energy graph. From these we identify the self-energy parts:

$$\Sigma^a_{G/H}(p) = (ZZ_\Delta - 1)p^2 = 0, \tag{4.19}$$

$$\Sigma^0_{G/H}(p) + \Sigma^r_{G/H}(p) = -i\hbar\left[\frac{(\lambda+\delta\lambda)v}{3}\right]^2 Z_\Delta^3 \mathcal{I}_{HG}(p). \tag{4.20}$$

Note that the Goldstone and Higgs self-energies are equal to this order as a consequence of the vertex Ward identity. This is essentially where our treatment differs from [9].

By using the auxiliary propagators to extract the divergences in $\mathcal{T}_{G/H}$ and $\mathcal{I}_{HG}(p)$ and absorbing them into the counterterms (see Appendix B), we find the finite equations of motion:

$$\Delta_G^{-1}(p) = p^2 - m^2 - \frac{\lambda}{6}v^2 - \frac{\hbar}{6}(N+1)\lambda\mathcal{T}_G^{\text{fin}} - \frac{\hbar}{6}\lambda\mathcal{T}_H^{\text{fin}} + i\hbar\left(\frac{\lambda v}{3}\right)^2[\mathcal{I}_{HG}^{\text{fin}}(p) - \mathcal{I}_{HG}^{\text{fin}}(m_G)], \tag{4.21}$$

$$\Delta_H^{-1}(p) = p^2 - m^2 - \frac{\lambda v^2}{3} - \frac{\lambda}{6}v^2 - \frac{\hbar}{6}(N+1)\lambda\mathcal{T}_G^{\text{fin}} - \frac{\hbar}{6}\lambda\mathcal{T}_H^{\text{fin}} + i\hbar\left(\frac{\lambda v}{3}\right)^2[\mathcal{I}_{HG}^{\text{fin}}(p) - \mathcal{I}_{HG}^{\text{fin}}(m_H)]. \tag{4.22}$$

The finite parts $\mathcal{T}^{\text{fin}}_{G/H}$ and $\mathcal{I}^{\text{fin}}_{HG}(p)$ are

$$\mathcal{I}^{\text{fin}}_{HG}(p) = \mathcal{I}_{HG}(p) - \mathcal{I}^\mu, \tag{4.23}$$

$$\mathcal{T}^{\text{fin}}_{G/H} = \mathcal{T}_{G/H} - \mathcal{T}^\mu + i(m^2_{G/H} - \mu^2)\mathcal{I}^\mu - \int_q i[\Delta^\mu(q)]^2\Sigma^\mu(q), \tag{4.24}$$

where the auxiliary quantities are

$$\mathcal{T}^\mu = \int_q i\Delta^\mu(q), \tag{4.25}$$

$$\mathcal{I}^\mu = \int_q [i\Delta^\mu(q)]^2, \tag{4.26}$$

$$\Sigma^\mu(q) = -i\hbar\left(\frac{\lambda v}{3}\right)^2\left[\int_\ell i\Delta^\mu(\ell)i\Delta^\mu(q+\ell) - \mathcal{I}^\mu\right]. \tag{4.27}$$

(For details see Appendix B.) These equations are the main result of this section. We expect they could be solved numerically using techniques similar to [21], though we leave the numerical implementation for later work.

B. Three-loop truncation

We consider now the three-loop truncation of the effective action. The vertex equation of motion is shown in Fig. 3, and we have already argued that the leading asymptotics at large momentum are captured by the auxiliary vertex defined by its equation of motion in Fig. 5. Subtracting these two equations we find that the right-hand side is finite (indeed the auxiliary vertices were constructed to guarantee this). Thus the problem of renormalizing the vertex equation of motion reduces to the problem of renormalizing the auxiliary vertex equation of motion.

It is temporarily more convenient to go back to the O(N) covariant form we had before introducing the SSB ansatz. Introduce the covariant auxiliary vertex V^μ_{abc} which is related to $\bar{V}^\mu$ and V^μ_N by an equation analogous to (3.13). Iterating the equation of motion, we find the solution

$$V^\mu_{abc} = \mathcal{K}_{abcdef}V_{0def}, \tag{4.28}$$

where the six-point kernel $\mathcal{K}_{abcdef}$ obeys the Bethe-Salpeter-like equation

$$\mathcal{K}_{abcdef} = \delta_{ad}\delta_{be}\delta_{cf} + \frac{1}{3!}\sum_\pi\left(-\frac{3i\hbar}{2}\right)\delta_{\pi(a)h} \times W_{\pi(b)\pi(c)kg}\Delta^\mu_{ki}\Delta^\mu_{gj}\mathcal{K}_{hijdef}, \tag{4.29}$$

where $\sum_\pi$ is a sum over permutations of the incoming legs. This equation is shown in Fig. 6. (4.29) can be written in a form that makes explicit all divergences (see Appendix C) and replaces the bare vertex W by a four-point kernel $\mathcal{K}^{(4)}_{abcd} \sim \lambda/(1+\lambda\mathcal{I}^\mu)$.

In fewer than four dimensions $\mathcal{K}^{(4)}_{abcd}$ is finite and every correction to the tree-level value is asymptotically subdominant. Thus the leading term at large momentum is the tree-level term and, instead of the full auxiliary vertex as we have defined it, one can simply take $V^\mu_{abc} = V_{0abc}$, dramatically simplifying the renormalization theory. A similar simplification happens to the auxiliary propagator due to

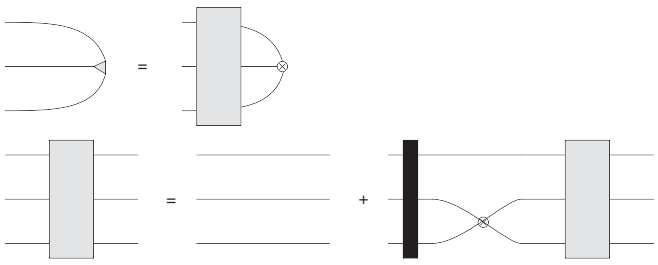

FIG. 6. Solution for the auxiliary vertex function in terms of a six-point kernel $\mathcal{K}_{abcdef}$ which is represented by the gray box (the indices run from top to bottom down the left side, then the right). The vertical black bar in the kernel equation of motion represents symmetrization of the external lines (with a factor of 1/3!).

the logarithmic (rather than quadratic) divergence of Φ_5-generated self-energy in $< 1+3$ dimensions. This confirms statements made in the literature (supported by numerical evidence though without proof, to our knowledge) to the effect that the asymptotic behavior of Green functions is free (e.g. [8]).

Unfortunately, the situation is much more difficult in four dimensions and the renormalization of the nPIEA for $n \geq 3$ in $d > 3$ remains an open problem, both in general and in the present case. The problem can be seen from the behavior of the auxiliary vertex which is discussed further in Appendix C. For the sake of obtaining analytical results we restrict the rest of this section to $< 1+3$ dimensions. The renormalization of the $1+3$ dimensional case is left to future work.

We derive the counterterms for $1+2$ dimensions in Appendix D. There are only two interesting comments about this derivation: the first is that we require an additional (nonuniversal) counterterm for the sunset graph linear in V; the second is that, consistent with the superrenormalizability of ϕ^4 theory in $1+2$ dimensions, only δm_1^2 is required to UV-renormalize the theory. Every other counterterm is finite and exists solely to maintain the pole condition for the Higgs propagator despite the vertex Ward identity. The resulting finite equations of motion are

$$\Delta_G^{-1} = -\left(\partial_\mu \partial^\mu + m^2 + \frac{\lambda}{6} v^2\right) - [\Sigma_G^0(p) - \Sigma_G^0(m_G)], \tag{4.30}$$

for the Goldstone propagator,

$$\bar{V} = -\frac{\lambda v}{3} + i\hbar[V_N(\bar{V})^2(\Delta_H)^2\Delta_G + (\bar{V})^3\Delta_H(\Delta_G)^2] + \frac{i\hbar\lambda}{6}[V_N(\Delta_H)^2 + (N+1)\bar{V}(\Delta_G)^2 + 4\bar{V}\Delta_G\Delta_H], \tag{4.31}$$

for the Higgs-Goldstone-Goldstone vertex, and

$$V_N = -\lambda v + i\hbar[(N-1)(\bar{V})^3(\Delta_G)^3 + (V_N)^3(\Delta_H)^3] + \frac{i\hbar\lambda}{2}[(N-1)\bar{V}\Delta_G\Delta_G + 3V_N(\Delta_H)^2], \tag{4.32}$$

for the triple Higgs vertex.

The finite Goldstone self-energy is

$$\begin{aligned} -\Sigma_G^0(p) = &-\frac{\hbar}{6}(N+1)\lambda(\mathcal{T}_G - \mathcal{T}^\mu) - \frac{\hbar}{6}\lambda(\mathcal{T}_H - \mathcal{T}^\mu) \\ &- i\hbar\left[-2\frac{\lambda v}{3} - \bar{V}\right]\Delta_H\Delta_G\bar{V} + \hbar^2[V_N(\bar{V})^3(\Delta_H)^3(\Delta_G)^2 + (\bar{V})^4\Delta_H\Delta_H(\Delta_G)^3] \\ &+ \frac{\hbar^2\lambda}{3}[\bar{V}V_N(\Delta_H)^3\Delta_G + (N+1)\bar{V}\,\bar{V}\,\Delta_H(\Delta_G)^3 + 3\bar{V}\,\bar{V}\,(\Delta_G)^2\Delta_H\Delta_H] \\ &+ \frac{\hbar^2\lambda^2}{18}[(N+1)(\Delta_G)^3 + \Delta_H\Delta_H\Delta_G - (N+2)\mathcal{B}^\mu], \end{aligned} \tag{4.33}$$

where the BBALL integral is $\mathcal{B}^\mu = \int_{qp} \Delta^\mu(q)\Delta^\mu(p)\Delta^\mu(p+q)$. The graph topologies are shown in Fig. 7. Finally, the Higgs equation of motion is

$$\Delta_H^{-1}(p) = (m_G^2 + \Sigma_G^0(m_H) - m_H^2) \times \frac{\bar{V}(p,-p,0)}{\bar{V}(m_H,-m_H,0)} + \Delta_G^{-1}(p). \tag{4.34}$$

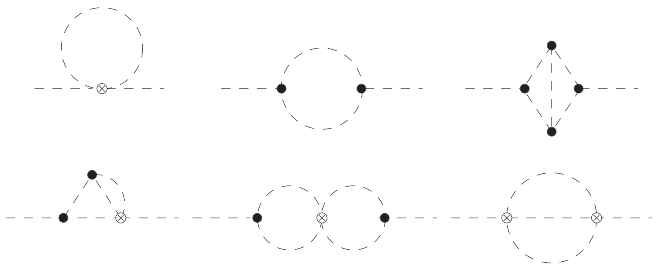

FIG. 7. Feynman graph topologies appearing in the self-energy function $\Sigma_G^0(p)$ in (4.33).

The unusual form of this equation is a result of the pole condition $\Delta_H^{-1}(m_H) = 0$. We defer the numerical implementation of these equations to future work.

V. SOLUTION OF THE HARTREE-FOCK APPROXIMATION

In the Hartree-Fock approximation one drops the $\mathcal{I}_{HG}(p)$ term in the two-loop equations of motion, or equivalently drops the sunset diagram. In this case the problem simplifies dramatically because the self-energy is momentum independent. The machinery of the auxiliary propagators introduced previously is now unnecessary and $\mathcal{T}_{G/H} = \mathcal{T}_{G/H}^\infty + \mathcal{T}_{G/H}^{\text{fin}}$ can be written as the sum of divergent and finite parts which can be evaluated in closed form. In the Matsubara formalism at finite temperature T the time contour is taken on the imaginary axis with periodic boundary conditions of period $-i\beta$, where $\beta = 1/T$. Integration over the timelike momentum

component p^0 becomes a sum over discrete Matsubara frequencies $\omega_n = 2\pi n/\beta$, $n = 0, \pm 1, \pm 2, \ldots$. Using standard tricks [14] the sum over frequencies can be performed, giving

$$\mathcal{T}^{\infty}_{G/H} = -\frac{m^2_{G/H}}{16\pi^2}\left[\frac{1}{\epsilon} - \gamma + 1 + \ln(4\pi)\right] + \mathcal{O}(\epsilon), \quad (5.1)$$

$$\mathcal{T}^{\mathrm{fin}}_{G/H} = \mathcal{T}^{\mathrm{vac}}_{G/H} + \mathcal{T}^{\mathrm{th}}_{G/H}, \quad (5.2)$$

$$\mathcal{T}^{\mathrm{vac}}_{G/H} = \frac{m^2_{G/H}}{16\pi^2}\ln\left(\frac{m^2_{G/H}}{\mu^2}\right), \quad (5.3)$$

$$\mathcal{T}^{\mathrm{th}}_{G/H} = \int_{\boldsymbol{q}} \frac{1}{\omega_{\boldsymbol{q}}}\frac{1}{e^{\beta\omega_{\boldsymbol{q}}} - 1}, \quad (5.4)$$

where the divergent and finite vacuum parts have been evaluated using $\overline{\mathrm{MS}}$ in $d = 4 - 2\epsilon$ dimensions at the renormalization point μ (note that [9] adopts a slightly different convention for $\mathcal{T}^{\mathrm{vac}}_{G/H}$ which amounts to a redefinition of μ not affecting physical results). $\gamma \approx 0.577$ is the Euler-Mascheroni constant. In the thermal part $\boldsymbol{q}$ is the spatial momentum vector and $\omega_{\boldsymbol{q}} = \sqrt{\boldsymbol{q}^2 + m^2_{G/H}}$. We substitute these expressions into the equations of motion (4.14)–(4.16) and demand that the kinematically distinct divergences proportional to v, $\mathcal{T}^{\mathrm{vac}}_{G/H}$, $\mathcal{T}^{\mathrm{th}}_{G/H}$ independently vanish. The other renormalization conditions are that residue of the pole of the propagator equals one, which requires $ZZ_\Delta = 1$, and that the tree-level relation $m^2_H = \frac{\lambda v^2}{3} + m^2_G$ holds at zero temperature. These conditions determine the renormalization constants

$$Z = Z_\Delta = 1, \quad (5.5)$$

$$\delta m^2_1 = \frac{(N+2)\hbar\lambda m^2}{96\pi^2\epsilon}\frac{(\epsilon\kappa + 1)}{1 - \frac{\hbar\lambda(N+2)(\epsilon\kappa+1)}{96\pi^2\epsilon}}, \quad (5.6)$$

$$\delta\lambda^A_1 = \frac{(N+4)\lambda}{(N+2)m^2}\delta m^2_1, \quad (5.7)$$

$$\delta\lambda^A_2 = \delta\lambda^B_2 = \frac{N+2}{N+4}\delta\lambda^A_1, \quad (5.8)$$

where $\kappa \equiv 1 - \gamma + \ln 4\pi \approx 2.95$. Note that the undetermined constant $\delta\lambda$ can be consistently set to zero at this order. The finite equations of motion are

$$m^2_G = m^2 + \frac{\lambda}{6}v^2 + \frac{\hbar\lambda}{6}(N+1)\mathcal{T}^{\mathrm{fin}}_G + \frac{\hbar\lambda}{6}\mathcal{T}^{\mathrm{fin}}_H, \quad (5.9)$$

$$m^2_H = \frac{\lambda v^2}{3} + m^2_G, \quad (5.10)$$

$$v m^2_G = 0. \quad (5.11)$$

Finally, if we demand the zero temperature tree-level relation $v^2(T=0) \equiv \bar{v}^2 = -6m^2/\lambda$ we must set the renormalization point $\mu^2 = \bar{m}^2_H \equiv m^2_H(T=0) = \lambda\bar{v}^2/3$.

The analogue of the equations of motion (5.9)–(5.11) corresponding to previous work on the symmetry improved 2PIEA is ([9,24] generalized to arbitrary N)

$$m^2_G = m^2 + \frac{\lambda}{6}v^2 + \frac{\hbar\lambda}{6}(N+1)\mathcal{T}^{\mathrm{fin}}_G + \frac{\hbar\lambda}{6}\mathcal{T}^{\mathrm{fin}}_H, \quad (5.12)$$

$$m^2_H = m^2 + \frac{\lambda}{2}v^2 + \frac{\hbar\lambda}{6}(N-1)\mathcal{T}^{\mathrm{fin}}_G + \frac{\hbar\lambda}{2}\mathcal{T}^{\mathrm{fin}}_H, \quad (5.13)$$

$$v m^2_G = 0. \quad (5.14)$$

Note that only the Higgs equation of motion differs, as expected. In the standard formalism without symmetry improvement one replaces (5.14) with

$$0 = v\left(m^2 + \frac{\lambda}{6}v^2 + \frac{\hbar\lambda}{6}(N-1)\mathcal{T}^{\mathrm{fin}}_G + \frac{\hbar\lambda}{2}\mathcal{T}^{\mathrm{fin}}_H\right). \quad (5.15)$$

These equations of motion, or *gap equations*, possess a phase transition and a critical point where $m^2_H = m^2_G = v^2 = 0$. Using the result for massless particles $\mathcal{T}^{\mathrm{th}}_{G/H}(m_{G/H} = 0) = T^2/12$, we find the same value of the critical temperature,

$$T_\star = \sqrt{\frac{12\bar{v}^2}{\hbar(N+2)}}, \quad (5.16)$$

independent of the formalism used. However, the order of the phase transition differs in the three cases. This stands in contrast to the large-N approximation, which correctly determines the order of the phase transition but gives a critical temperature larger by a factor of $\sqrt{3/2} + \mathcal{O}(N^{-1})$ (see [24,25]).

We present numerical solutions of equations (5.9)–(5.15) with $N = 4$, $v = 93$ MeV and $\bar{m}_H = 500$ MeV. These values are chosen to represent the low energy mesonic sector of QCD, and to enable direct comparison with [24]. Our results are also closely comparable with [25], though they take $\bar{m}_H \approx 600$ MeV. The solution is implemented in Python as an iterative root finder based on *scipy.optimize.root* [26] with an estimated Jacobian or, if that fails to converge, a direct iteration of the gap equations. The Bose-Einstein integrals in (5.4) can be precomputed to save time. We show the results for the scalar field v, Higgs mass m_H and Goldstone mass m_G in Figs. 8, 9, and 10, respectively.

Figure 8 shows $v(T)$, the order parameter of the phase transition. Below the critical temperature there is a broken

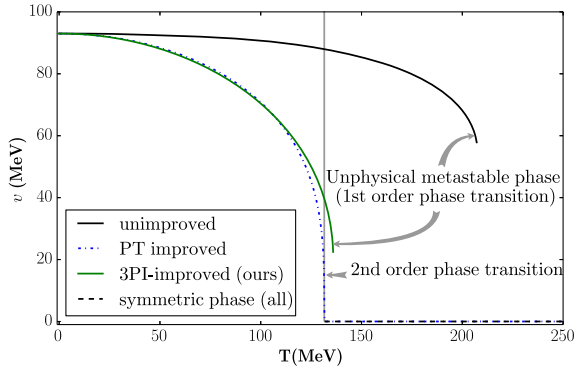

FIG. 8 (color online). Expectation value of the scalar field $v = \langle\phi\rangle$ as a function of temperature T computed in the Hartree-Fock approximation using the unimproved 2PIEA (solid black), the Pilaftsis and Teresi symmetry improved 2PIEA (dash dotted blue) and our symmetry improved 3PIEA (solid green). In the symmetric phase (dashed black) all methods agree. The vertical grey line at $T \approx 131.5$ MeV corresponds to the critical temperature which is the same in all methods.

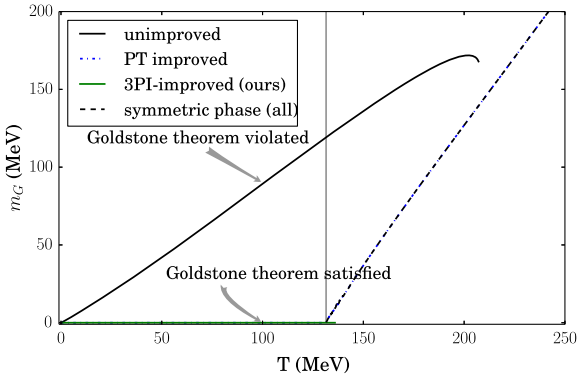

FIG. 10 (color online). The Goldstone mass m_G as a function of temperature T computed in the Hartree-Fock approximation using the unimproved 2PIEA (solid black), the Pilaftsis and Teresi symmetry improved 2PIEA (dash dotted blue) and our symmetry improved 3PIEA (solid green). In the symmetric phase (dashed black) all methods agree. The vertical grey line at $T \approx 131.5$ MeV corresponds to the critical temperature which is the same in all methods.

phase with $v \neq 0$, but the symmetry is restored when $v = 0$ above the critical temperature. Note, however, that the unimproved and symmetry improved 3PIEA have unphysical metastable broken phases at $T > T_\star$, signalling a first-order phase transition. The symmetry improved 2PIEA correctly predicts the second-order nature of the phase transition. Though unphysical, the symmetry improved 3PIEA behavior is much more reasonable than the unimproved 2PIEA: the strength of the first-order phase transition is reduced and the metastable phase ceases to exist at a temperature much closer to the critical temperature than for the unimproved 2PIEA. Figure 9 shows the Higgs mass $m_H(T)$. The phase transition behavior above is seen again,

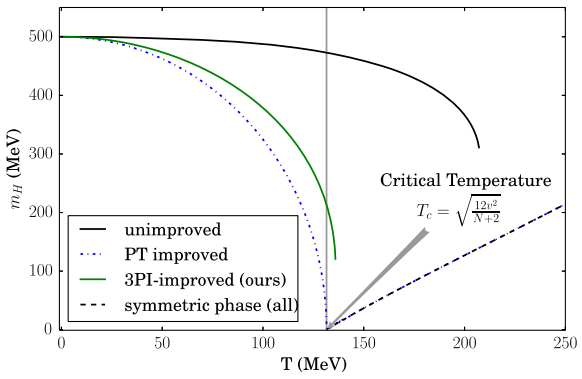

FIG. 9 (color online). The Higgs mass m_H as a function of temperature T computed in the Hartree-Fock approximation using the unimproved 2PIEA (solid black), the Pilaftsis and Teresi symmetry improved 2PIEA (dash dotted blue) and our symmetry improved 3PIEA (solid green). In the symmetric phase (dashed black) all methods agree. The vertical grey line at $T \approx 131.5$ MeV corresponds to the critical temperature which is the same in all methods.

and again all three methods agree in the symmetric phase, giving the usual thermal mass effect. Finally, Fig. 10 shows the Goldstone boson mass. The unimproved 2PIEA strongly violates the Goldstone theorem, but both symmetry improvement methods satisfy it as expected. Note that the Goldstone theorem is even satisfied in the unphysical metastable phase predicted by the symmetry improved 3PIEA. All three methods correctly predict $m_G = m_H$ in the symmetric phase.

VI. TWO DIMENSIONS AND THE COLEMAN-MERMIN-WAGNER THEOREM

Recall that the Coleman-Mermin-Wagner theorem [27], which has been interpreted as a breakdown of the Goldstone theorem [28], is a general result stating that the spontaneous breaking of a continuous symmetry is impossible in $d = 2$ or $d = 1 + 1$ dimensions. This occurs due to the infrared divergence of the massless scalar propagator in two dimensions. We show that the symmetry improved gap equations satisfy this theorem despite the direct imposition of Goldstone's theorem. Thus symmetry improvement passes another test that any robust quantum field theoretical method must satisfy. (Note that symmetry improvement is not *required* to obtain consistency of *n*PIEA with the Coleman-Mermin-Wagner theorem, but neither does it ruin it.)

The general statement of the result is that $\int_x \Sigma(x,0)$ diverges whenever massless particles appear in loops in $d = 2$, thus, by (2.17) and (3.19) $v = 0$ and a mass gap is generated. We will show this explicitly using the Hartree-Fock gap equations (5.9)–(5.11), where in two dimensions,

$$\mathcal{T}_a^{\text{vac}}(\overline{\text{MS}}) = -\frac{1}{4\pi}\ln\left(\frac{m_a^2}{\mu^2}\right). \tag{6.1}$$

(Note that the renormalization can be carried through without difficulty in two dimensions. Only the δm_1^2 counterterm is needed.) We must show that the gap equations possess no solution for $m_G^2 = 0$. It is clear that if $v \neq 0$, $\mathcal{T}_G^{\rm vac}$ diverges as $m_G^2 \to 0$ if we take μ as a constant, and $\mathcal{T}_H^{\rm vac}$ diverges if we take $\mu^2 \propto m_G^2$ as $m_G^2 \to 0$. Either way there is no solution. At finite temperature the Bose-Einstein integral $\mathcal{T}_a^{\rm th}$ also has an infrared divergence as $m_a \to 0$ which does not cancel against the singularity of the vacuum term. It can be shown that the singularity is due to the Matsubara zero mode.

For $v = 0$ on the other hand, the gap equations reduce to

$$m_H^2 = m_G^2 = m^2 - \frac{1}{4\pi}\frac{\hbar}{6}(N+2)\lambda \ln\left(\frac{m_G^2}{\mu^2}\right), \tag{6.2}$$

which always has a positive solution. If $m^2 > 0$ then one can choose the renormalization point $\mu^2 = m_G^2$ so that the tree-level relationship $m_G^2 = m^2$ holds. If $m^2 < 0$ a positive mass is dynamically generated and one requires a renormalization point $\mu^2 > m_G^2 \exp(\frac{24\pi|m^2|}{\hbar(N+2)\lambda})$ nonperturbatively large in the ratio $\lambda/|m^2|$, reflecting the fact that perturbation theory is bound to fail in this case.

VII. OPTICAL THEOREM AND DISPERSION RELATIONS

In this section we examine the analytic structure of propagators and self-energies in the symmetry improved 3PI formalism. A physical quantity of particular interest is the decay width Γ_H of the Higgs, which is dominated by decays to two Goldstones. Γ_H is given by the optical theorem in terms of the imaginary part of the self-energy evaluated on-shell (see, e.g. [29], Chap. 7):

$$-m_H\Gamma_H = \mathrm{Im}\Sigma_H(m_H). \tag{7.1}$$

(This is valid so long as $\Gamma_H \ll m_H$; otherwise, the full energy dependence of $\Sigma_H(p)$ must be taken into account.) The standard one-loop perturbative result gives

$$\Gamma_H = \frac{N-1}{2}\frac{\hbar}{16\pi m_H}\left(\frac{\lambda v}{3}\right)^2, \tag{7.2}$$

which comes entirely from the Goldstone loop sunset graph. Each part of this expression has a simple interpretation in relation to the tree-level decay graph (Fig. 11). The $N-1$ is due to the sum over final state Goldstone flavors, the factor of $1/2$ is due to the Bose statistics of the two particles in the final state, the $\hbar/16\pi m_H$ is due to the final state phase space integration and the $(\lambda v/3)^2$ is the absolute square of the invariant decay amplitude.

The Hartree-Fock approximation fails to reproduce this result regardless of the use or not of symmetry improvement. This is because there is no self-energy apart from a mass correction. Thus the Hartree-Fock approximation always predicts that the Higgs is stable. Attempts to repair the Hartree-Fock approximation through the use of an external propagator lead to a nonzero but still incorrect result. This is because an unphysical value of m_G still appears in loops. Satisfactory results are obtained within the symmetry improved 2PI formalism for both on- and off-shell Higgs [9]. Here we show that the symmetry improved 3PIEA can not yield a satisfactory value for Γ_H at the two-loop level.

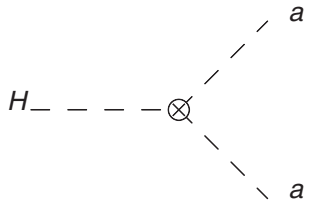

FIG. 11. Tree level of decay of the Higgs (H) to two Goldstone bosons $a = 1, \cdots, N-1$.

From (4.22),

$$\begin{aligned}\mathrm{Im}\Sigma_H(p) &= \frac{\hbar}{6}(N+1)\lambda \mathrm{Im}\mathcal{T}_G^{\rm fin} + \frac{\hbar}{6}\lambda \mathrm{Im}\mathcal{T}_H^{\rm fin} \\ &\quad - \hbar\left(\frac{\lambda v}{3}\right)^2 \mathrm{Im}[i\mathcal{I}_{HG}^{\rm fin}(p)] \\ &= \frac{\hbar}{6}(N+1)\lambda \mathrm{Im}\mathcal{T}_G + \frac{\hbar}{6}\lambda \mathrm{Im}\mathcal{T}_H \\ &\quad - \hbar\left(\frac{\lambda v}{3}\right)^2 \mathrm{Im}[i\mathcal{I}_{HG}(p)],\end{aligned} \tag{7.3}$$

which can be written in terms of the unsubtracted $\mathcal{T}_{G/H}$ and $\mathcal{I}_{HG}$ because all of the subtractions are manifestly real. Now we show that $\mathrm{Im}\mathcal{T}_{G/H} = 0$. To do this we introduce the Källén-Lehmann spectral representation of the propagators [30],

$$\Delta_{G/H}(q) = \int_0^\infty \mathrm{d}s \frac{\rho_{G/H}(s)}{q^2 - s + i\epsilon}, \tag{7.4}$$

where the spectral densities $\rho_{G/H}(s)$ are real and positive for $s \geq 0$ and obey the sum rule

$$\int_0^\infty \mathrm{d}s \rho_{G/H}(s) = (ZZ_\Delta)^{-1} = 1, \tag{7.5}$$

where the last equality holds at two-loop order (we have adapted the standard formula to our renormalization scheme).

(Note that this standard theory actually conflicts with the asymptotic $p^2(\ln p^2)^{c_1}$ form assumed for the self-energy when the Φ_5 graph is included, so that our argument must be refined at the three-loop level. The essential problem is that the self-consistent nPI propagator is not resumming

large logarithms. However, it seems unlikely that a refinement of the argument to account for this fact will change the qualitative conclusions of this section since, as will be shown shortly, the predicted Γ_H is wrong by group theory factors in addition to the $\mathcal{O}(1)$ factors which could be compensated by a modification of $\rho_{G/H}$.)

Then,

$$\mathrm{Im}\int_q i\int_0^\infty \mathrm{d}\mu^2 \frac{\rho_{G/H}(\mu^2)}{q^2-\mu^2+i\epsilon} = \mathrm{Im}\int_0^\infty \mathrm{d}\mu^2 \rho_{G/H}(\mu^2)\mathcal{T}^\mu = 0. \tag{7.6}$$

This allows us to obtain a dispersion relation relating the real and imaginary parts of the self-energies,

$$0 = \mathrm{Im}\int_q i\frac{1}{q^2-m_{G/H}^2-\Sigma_{G/H}(q)} = \int_q \frac{q^2-m_{G/H}^2-\mathrm{Re}\Sigma_{G/H}(q)}{[q^2-m_{G/H}^2-\mathrm{Re}\Sigma_{G/H}(q)]^2+[\mathrm{Im}\Sigma_{G/H}(q)]^2}. \tag{7.7}$$

Finally, we have left to compute $\mathrm{Im}[i\mathcal{I}_{HG}(p)]$ which can be written

$$\begin{aligned}\mathrm{Im}[i\mathcal{I}_{HG}(p)] &= \mathrm{Im}i\int_q\int_0^\infty \mathrm{d}s_1\int_0^\infty \mathrm{d}s_2 \frac{i\rho_N(s_1)}{q^2-s_1+i\epsilon}\frac{i\rho_G(s_2)}{(p-q)^2-s_2+i\epsilon}\\ &= \mathrm{Im}i\int_0^\infty \mathrm{d}s_1\int_0^\infty \mathrm{d}s_2\rho_N(s_1)\rho_G(s_2)\int_q \frac{i}{q^2-s_1+i\epsilon}\frac{i}{(p-q)^2-s_2+i\epsilon}\\ &= \frac{1}{16\pi^2}\int_0^\infty \mathrm{d}s_1\int_0^\infty \mathrm{d}s_2\rho_N(s_1)\rho_G(s_2)\mathrm{Im}\int_0^1 \mathrm{d}x \ln\left(\frac{\mu^2}{-x(1-x)p^2+xs_1+(1-x)s_2-i\epsilon}\right).\end{aligned} \tag{7.8}$$

The imaginary part of the x integral is only nonzero for $\sqrt{s_1}+\sqrt{s_2}<\sqrt{p^2}$. We denote the region of $s_{1,2}$ integration by Ω. Then the imaginary part of the x integral can be evaluated straightforwardly, giving

$$\begin{aligned}\mathrm{Im}[i\mathcal{I}_{HG}(p)] = \frac{1}{16\pi p^2}\int_\Omega \mathrm{d}s_1\mathrm{d}s_2\rho_N(s_1)\rho_G(s_2)&\\ \times\sqrt{p^2-(\sqrt{s_1}+\sqrt{s_2})^2}&\\ \times\sqrt{p^2-(\sqrt{s_1}-\sqrt{s_2})^2}.&\end{aligned} \tag{7.9}$$

Now, since the each term of the integrand is positive and the square root is $\le p^2$, we have

$$\mathrm{Im}[i\mathcal{I}_{HG}(p)] \le \frac{1}{16\pi}\int_\Omega \mathrm{d}s_1\mathrm{d}s_2\rho_N(s_1)\rho_G(s_2) \le \frac{1}{16\pi}, \tag{7.10}$$

using the sum rule for $\rho_{N/G}(s)$. Finally, we have

$$\Gamma_H \le \frac{\hbar}{16\pi m_H}\left(\frac{\lambda v}{3}\right)^2, \tag{7.11}$$

which is smaller than the expected value for all $N>3$. $N=2$ and 3 are cases where one could possibly obtain an (accidentally) reasonable result, depending on the precise form of the spectral functions, but it is clear that one should not generically expect a correct prediction of Γ_H from the symmetry improved 3PIEA at two loops. The source of the problem is the derivation of the two-loop truncation where we dropped the vertex correction term in (3.24), resulting in a truncation of the true Ward identity (3.20) that keeps the one-loop graphs in Σ_G but not in $\bar{V}$. The diagram contributing to Γ_H above is thus the Goldstone self-energy shown in Fig. 12 which has the incorrect kinematics and lacks the required group theory $(N-1)$ and Bose symmetry $(1/2)$ factors as well. In fact, a perturbative evaluation of Fig. 12 gives $\Gamma_H=0$ due to the threshold at $p^2=m_H^2$! What we have shown is that no matter the form of the exact spectral functions, there cannot be a nonperturbative enhancement of this graph large enough to give the correct Γ_H for $N>3$. The neglected vertex corrections give a leading $\mathcal{O}(\hbar)$ contribution to Γ_H which must be included.

Now we consider the three-loop truncation of the symmetry improved 3PIEA. Since one-loop vertex corrections appear at this order we expect that Γ_H should be correct at least to $\mathcal{O}(\hbar)$. Since the previous result was incorrect by group theory factors already at $\mathcal{O}(\hbar)$ our task simplifies to seeking only the $\mathcal{O}(\hbar)$ decay width, and so we make use of only the one-loop terms in the Higgs equation of motion, which are displayed in Fig. 13. Furthermore, by

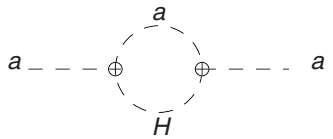

FIG. 12. The self-energy diagram from (4.22) which, due to the inconsistent truncation of the Ward identity, gives the incorrect absorptive part to the Higgs propagator in the two-loop truncated symmetry improved 3PIEA. $a=1,\cdots,N-1$ labels Goldstone boson lines and H labels the Higgs boson line.

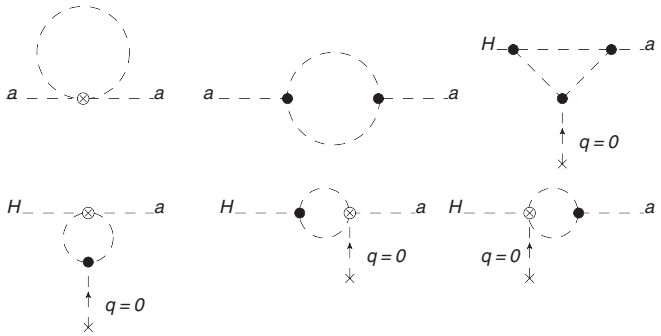

FIG. 13. One-loop contribution to the Higgs self-energy. The tadpole and sunset graphs are from the Higgs self-energy Σ_G, while the four remaining terms come from vertex corrections via the Ward identity (3.20). The momentum incoming from the lower Goldstone leg is zero, and the crossed vertex represents a factor of v.

iterating the equations of motion we may replace all propagators and vertices by their perturbative values to $\mathcal{O}(\hbar)$. This will leave out contributions of higher-order decay processes such as $H \to GGGG$. We leave the numerical task of computing the exact decay width predicted by the symmetry improved 3PIEA to future work.

The contributions of the various terms in Fig. 13 to the imaginary part of Σ_H can be determined using Cutkosky cutting rules [29]. In particular, the Hartree-Fock diagram and the first bubble vertex correction diagram (left diagram, bottom row Fig. 13) have no cuts such that all cut lines can be put on shell. Also, cuts through intermediate states with both Goldstone and Higgs lines contribute to the process $H \to HG$, which vanishes due to the zero phase space at threshold. This means we can drop the sunset diagram and the last bubble vertex correction (right diagram, bottom row Fig. 13). Similarly cuts through two intermediate Higgs lines can be dropped since $H \to HH$ is impossible on shell. This mean we can drop the contributions to the triangle and remaining bubble diagram where the leftmost vertex is V_N rather than $\bar{V}$. The contributions we are interested in can now be displayed explicitly:

$$\begin{aligned}-\Sigma_H &\supset \bar{V} v \\ &\supset v\left[i\hbar\left(-\frac{\lambda v}{3}\right)^3 \int_\ell \frac{1}{(\ell-p)^2 - m_G^2 + i\epsilon} \right. \\ &\times \frac{1}{\ell^2 - m_G^2 + i\epsilon}\frac{1}{\ell^2 - m_H^2 + i\epsilon} \\ &+ \frac{i\hbar\lambda}{6}(N+1)\left(-\frac{\lambda v}{3}\right) \\ &\left.\times \int_\ell \frac{1}{(\ell-p)^2 - m_G^2 + i\epsilon}\frac{1}{\ell^2 - m_G^2 + i\epsilon}\right], \end{aligned} \tag{7.12}$$

where the first and second term are the triangle and bubble graphs, respectively. We now cut the Goldstone lines by replacing each cut propagator $(p^2 - m_G^2 + i\epsilon)^{-1} \to -2\pi i\delta(p^2 - m_G^2)$ to give $-2i\mathrm{Im}\Sigma_H$ (because the cutting rules give the *discontinuity* of the diagram, which is $2i$ times the imaginary part), yielding

$$\begin{aligned}-2i\mathrm{Im}\Sigma_H &\supset -i\hbar v\left[\left(-\frac{\lambda v}{3}\right)^3 \frac{1}{-m_H^2} + \frac{\lambda}{6}(N+1)\left(-\frac{\lambda v}{3}\right)\right] \\ &\times \int_\ell 2\pi\delta((\ell-p)^2)2\pi\delta(\ell^2) \\ &= i\hbar\frac{\lambda^2 v^2}{3^2 2}(N-1)\int_\ell 2\pi\delta((\ell-p)^2)2\pi\delta(\ell^2). \end{aligned} \tag{7.13}$$

The integral can be evaluated by elementary techniques, giving

$$\begin{aligned}&\int_\ell 2\pi\delta((\ell-p)^2)2\pi\delta(\ell^2) \\ &= \frac{1}{4\pi^2}\int \mathrm{d}^4\ell \times \delta(\ell^2 - 2\ell\cdot p + p^2)\delta(\ell^2) \\ &= \frac{1}{4\pi^2}\int \mathrm{d}\ell_0 \mathrm{d}l 4\pi l^2 \times \delta(-2\ell_0 m_H + m_H^2)\delta(\ell_0^2 - l^2) \\ &= \frac{1}{\pi}\int \mathrm{d}l l^2 \frac{1}{2m_H}\frac{\delta(\frac{m_H}{2} - l)}{2\frac{m_H}{2}} \\ &= \frac{1}{8\pi}, \end{aligned} \tag{7.14}$$

and finally

$$-\mathrm{Im}\Sigma_H(m_H) = \frac{N-1}{2}\frac{\hbar}{16\pi}\left(\frac{\lambda v}{3}\right)^2 + \mathcal{O}(\hbar^2). \tag{7.15}$$

This exactly matches the expected Γ_H, including group theory and Bose symmetry factors. The full nonperturbative solution will give corrections to this accounting for loop corrections as well as cascade decay processes $H \to GG \to (GG)^2 \to \cdots$. We leave the evaluation of this to future work; however, we have shown that the one-loop vertex corrections are required to get the correct Γ_H at leading order.

VIII. DISCUSSION

The symmetry improvement formalism of Pilaftsis and Teresi is able to enforce the preservation of global symmetries in two particle irreducible effective actions, allowing among other things the accurate description of phase transitions in strongly coupled theories using numerical methods that are relatively cheap compared to lattice methods. As an example of this, during the preparation of this manuscript it was shown that the symmetry improved 2PIEA solves problems with infrared divergences of the standard model effective potential due to massless

Goldstone bosons [31], though that study was carried out without the gauge sector. It also shows that the symmetry improved 2PIEA performs better than an *ad hoc* resummation scheme proposed in the prior literature. This is heartening, though not wholly surprising due to the inherent self-consistency of nPIEA, a topic we plan to discuss in a forthcoming publication.

However, the development of a first principles nonperturbative kinetic theory for the gauge theories of real physical interest requires the use of n-particle irreducible effective actions with $n \geq 3$. We have taken a step in this direction by extending the symmetry improvement formalism to the 3PIEA for a scalar field theory with spontaneous breaking of a global $\mathrm{O}(N)$ symmetry. We found that an extra Ward identity involving the vertex function must be imposed. Since the constraints are singular this required a careful consideration of the variational procedure, namely one must be careful to impose constraints in a way that satisfies d'Alembert's principle. Once this is done the theory can be renormalized in a more or less standard way, though the counterterms differ in value from the unimproved case. We derived finite equations of motion and counterterms for the Hartree-Fock truncation, two-loop truncation, and three-loop truncation of the effective action.

We found several important qualitative results. First, symmetry improvement breaks the equivalence hierarchy of nPIEA. Second, the numerical solution of the Hartree-Fock truncation gave mixed results: Goldstone's theorem was satisfied, but the order of the phase transition was incorrectly predicted to be weakly first order (though there was still a large quantitative improvement over the unimproved 2PIEA case). Third, the two-loop truncation incorrectly predicts the Higgs decay width as a consequence of the optical theorem, though the three-loop truncation gives the correct value, at least to $\mathcal{O}(\hbar)$. These results could be considered strong circumstantial evidence that one should not apply symmetry improvement to nPIEA at a truncation to less than n loops. One could test this conjecture further by, for example, computing the symmetry improved 4PIEA. We predict that unsatisfactory results of some kind will be found for any truncation of this to < 4 loops.

Our renormalization of the theory at two and three loops was performed in vacuum. The only finite temperature computation performed here was for the Hartree-Fock approximation. The extension of the two- or three-loop truncations to finite temperature, or an extension to nonequilibrium situations, will require a much heavier numerical effort than what we have attempted. It would also be interesting to compare the self-consistent Higgs decay rate in the symmetry improved 2PI and 3PI formalisms. We leave these investigations to future work. Similarly, we presented analytical results for the renormalization of the three-loop truncation only in $1+2$ dimensions, since the renormalization was not analytically tractable in $1+3$ dimensions. This is also left to future work. The general renormalization theory presented here, based on counterterms, is difficult to use in practice. It will be interesting to see if symmetry improvement could work along with the counterterm-free functional renormalization group approach [32]. Such an approach may not be easier to set up in the first place, but once developed would likely be easier to extend to higher-loop order and n than the current method. Of course it will be interesting to see if this work can be extended to gauge symmetries and, eventually, the standard model of particle physics. If successful, such an effort could serve to open a new window to the nonperturbative physics of these theories in high temperature, high density and strong coupling regimes.

ACKNOWLEDGMENTS

We thank Daniele Teresi for clarifying comments concerning [9] and Peter Drummond for useful discussions relating to asymptotic series and summability.

APPENDIX A: THE D'ALEMBERT FORMALISM

The assumption that $\delta f/\delta \mathcal{W}_2$ can be consistently taken to be constant requires explanation. Constrained Lagrangian problems are generally underspecified unless one invokes some principle like d'Alembert's principle (that the constraint forces are "ideal"; i.e., they do no work on the system) to specify the constraint forces. Note that while it is usually stated that enforcing constraints through Lagrange multipliers is equivalent to applying d'Alembert's principle, this is no longer automatically the case if the constraints involve a singular limit as happens in the field theory case. This leads to a real ambiguity in the procedure which requires the analyst to input physical information to resolve it. In the case of mechanical systems the analyst is expected to be able to furnish the correct form of the constraints by inspection of the system. However, the interpretation of "work" and "constraint force" in the field theory case is subtle and the appropriate generalization is not obvious. Here we argue, by way of a simple mechanical analogy, that the procedure which leads to the maximum simplification of the equations of motion is the correct field theory analogue of d'Alembert's principle in mechanics.

d'Alembert's principle is empirically verifiable for a given mechanical system, but for us it forms part of the *definition* of our approximation scheme, which we refer to as the "d'Alembert formalism." The result of Sec. III was a set of unambiguous f-independent equations of motion and constraint at some fixed order of the loop expansion, say l loops. The use of any other limiting procedure requires the analyst to specify a spacetime function's worth of data ahead of time, representing the "work" that the constraint forces do. The resulting equations of motion represent a different formulation of the system and will have a different solution depending on the choice of "work" function.

Imagine that we are competing against another analyst to find the most accurate solution for a particular system. It is possible that a competing smart analyst could choose a work function that results in a more accurate solution than ours, also working at l loops. However, we could beat the other analyst by working in the d'Alembert formalism but at higher loop order. We conjecture that the optimum choice of work function (in the sense of guaranteeing the optimum accuracy of the resulting solution of the l-loop equations) is merely a clever repackaging of information contained in $> l$-loop corrections. (We have no proof of this conjecture. Indeed it is hard to see if any alternative to the d'Alembert formalism is practicable.) Thus we choose the d'Alembert formalism, which has the virtue of being a definite procedure requiring little cleverness from the analyst, at the cost of potentially having a suboptimal accuracy for a given loop order.

To illustrate the connection with a mechanics problem consider a classical particle in two dimensions constrained to $x^2 + y^2 = r^2$. The motion is uniformly circular:

$$\begin{pmatrix} x \\ y \end{pmatrix} = r \begin{pmatrix} \cos(\omega t + \phi) \\ \sin(\omega t + \phi) \end{pmatrix}. \tag{A1}$$

The action is

$$S = \int L \mathrm{d}t - \lambda f[w], \tag{A2}$$

$$L = \frac{1}{2} m(\dot{x}^2 + \dot{y}^2), \tag{A3}$$

where the constraint is $w(t) = x(t)^2 + y(t)^2 - r^2 = 0$ and $f[w] = 0$ if $w(t) = 0$. The equations of motion are

$$m\ddot{x}(t) = -2\lambda \frac{\delta f}{\delta w(t)} x(t), \tag{A4}$$

$$m\ddot{y}(t) = -2\lambda \frac{\delta f}{\delta w(t)} y(t). \tag{A5}$$

In this mechanics problem we could set $f[w] = \int w(t)\mathrm{d}t$ and carry through the problem in the standard way without any complications. But to mimic the field theory case, where a limiting procedure is required, we take $f[w] = \int w(t)^2 \mathrm{d}t$. In this case,

$$\frac{\delta f}{\delta w(t)} = 2w(t) \to 0 \quad \text{as } w \to 0. \tag{A6}$$

This requires $\lambda \to \infty$ such that $\lambda \delta f/\delta w$ approaches a finite limit. Importantly, it must approach a t independent limit, otherwise an unspecified function of time enters the equations of motion: $m\ddot{x}(t) = -k(t)x(t)$, etc. This limit can be achieved by restricting the class of variations considered. Let $x(t) = r(t)\cos\theta(t)$ and $y(t) = r(t)\sin\theta(t)$, where $\delta r(t) = r(t) - r$ parametrizes deviations from the constraint surface. Then $w(t) = 2r\delta r(t) + \mathcal{O}(\delta r^2)$. We want $\dot{w}(t) = 0$ which is obviously satisfied by $\delta r(t) = \delta r$.

We are arguing that we only consider variations of this restricted form. The variations along the constraint surface [i.e. variations of $\theta(t)$] are unrestricted as they should be. Only variations orthogonal to the constraint surface are restricted. This is equivalent to d'Alembert's principle. To see this we compute the second derivative of r^2 to obtain $\dot{\theta}^2 - k = \frac{\ddot{r}}{r}$. When the constraint is enforced $\ddot{r} = 0$, hence $\dot{k} \neq 0$ implies $\ddot{\theta} \neq 0$: the constraint forces are causing angular accelerations, doing work on the particle. At constant radius, the centripetal force only changes if the angular velocity changes.

In the field theory case we have (3.56). For any given value of $\bar{V}$ and Δ_G, only one value of Δ_H satisfies the constraint, given by

$$\Delta_H^{-1\star}(x,y) = \int_z \bar{V}(x,y,z)v + \Delta_G^{-1}(x,y), \tag{A7}$$

where the $\star$ denotes the constraint solution. This is a holonomic constraint: in principle, we could substitute this into the effective action directly and not worry about Lagrange multipliers at all (this is very messy analytically, though it may be numerically feasible). We suggest that one restrict variations of Δ_H^{-1} to be of the form $\Delta_H^{-1\star}(x,y) + \delta k$, where δk is a spacetime independent constant. This way we guarantee

$$\frac{\delta f}{\delta \mathcal{W}_2(x,y)} = 2\mathcal{W}_2(x,y) = -2\delta k = \text{const}, \tag{A8}$$

and all the desired simplifications go through. Variations of the other variables are unrestricted. Because the constraint force $B\delta f/\delta \mathcal{W}_2$ disappears from the Δ_G, $\bar{V}$ and V_N equations of motion the constraint "does no work" on these variables, and the other variables (v and Δ_H) are determined solely by the constraint equations. This seems a fitting field theory analogy for d'Alembert's principle.

APPENDIX B: DERIVING COUNTERTERMS FOR TWO-LOOP TRUNCATIONS

In this section we derive the counterterms required to renormalize the 3PIEA and equations of motion in the two-loop truncation as discussed in Sec. IV A. Substituting the expressions for bare fields and parameters in terms of the renormalized fields and parameters according to (4.9)–(4.13) gives the renormalized effective action

$$\Gamma^{(3)} = \int_x \left(-Z_\Delta^{-1}\frac{m^2+\delta m_0^2}{2}v^2 - \frac{\lambda+\delta\lambda_0}{4!}v^4\right) + \frac{i\hbar}{2}(N-1)\mathrm{Tr}\ln(Z^{-1}Z_\Delta^{-1}\Delta_G^{-1}) + \frac{i\hbar}{2}\mathrm{Tr}\ln(Z^{-1}Z_\Delta^{-1}\Delta_H^{-1})$$
$$-\frac{i\hbar}{2}(N-1)\mathrm{Tr}\left[\left(ZZ_\Delta\partial_\mu\partial^\mu + m^2 + \delta m_1^2 + Z_\Delta\frac{\lambda+\delta\lambda_1^A}{6}v^2\right)\Delta_G\right]$$
$$-\frac{i\hbar}{2}\mathrm{Tr}\left[\left(ZZ_\Delta\partial_\mu\partial^\mu + m^2 + \delta m_1^2 + Z_\Delta\frac{3\lambda+\delta\lambda_1^A+2\delta\lambda_1^B}{6}v^2\right)\Delta_H\right] + \Gamma_3^{(3)}, \tag{B1}$$

which agrees with the nongraphical terms of [9] Eq. (4.4) upon setting $N=2$, dropping an irrelevant constant $\propto \mathrm{Tr}\ln Z^{-1}$ and noting our different conventions ($m^2_{\mathrm{here}} = -m^2_{\mathrm{PT}}$ and $\lambda_{\mathrm{here}} = 6\lambda_{\mathrm{PT}}$). The $\delta\lambda$ terms can be derived by substituting $\lambda_B\varphi_{Bc}\varphi_B^c \to Z^{-2}(\lambda+\delta\lambda_1^A)Zv^2$ and $\lambda_B\varphi_{Ba}\varphi_{Bb} \to Z^{-2}(\lambda+\delta\lambda_1^B)Zv^2\delta_{aN}\delta_{bN}$ into the definition of Δ_{0ab}^{-1}.

The graph functional becomes

$$\Gamma_3^{(3)} = \Phi_1 - \frac{\hbar^2(\lambda+\delta\lambda)v}{3!}Z_V Z_\Delta^3\int_{xyzw}\Delta_H(x,y)[\Delta_H(x,z)\Delta_H(x,w)V_N(y,z,w)$$
$$+ (N-1)\Delta_G(x,z)\Delta_G(x,w)\bar{V}(y,z,w)] - \Phi_2 + \mathcal{O}(\hbar^3), \tag{B2}$$

with

$$\Phi_1 = \frac{\hbar^2}{24}[(N+1)\lambda + (N-1)\delta\lambda_2^A + 2\delta\lambda_2^B]Z_\Delta^2(N-1)\Delta_G\Delta_G$$
$$+\frac{\hbar^2}{24}[3\lambda+\delta\lambda_2^A+2\delta\lambda_2^B]Z_\Delta^2\Delta_H\Delta_H + \frac{\hbar^2}{24}2(\lambda+\delta\lambda_2^A)Z_\Delta^2(N-1)\Delta_G\Delta_H \tag{B3}$$

$$\Phi_2 = \frac{\hbar^2}{4}(N-1)Z_V^2Z_\Delta^3\bar{V}\,\bar{V}\,\Delta_H\Delta_G\Delta_G + \frac{\hbar^2}{12}Z_V^2Z_\Delta^3V_NV_N\Delta_H\Delta_H\Delta_H. \tag{B4}$$

The $\delta\lambda_2^{A/B}$ terms can be found from substituting $\lambda_B\Delta_{Baa}\Delta_{Bbb} \to Z^{-2}(\lambda+\delta\lambda_2^A)Z^2Z_\Delta^2\Delta_{aa}\Delta_{bb}$ and $\lambda_B\Delta_{Bab}\Delta_{Bba} \to Z^{-2}(\lambda+\delta\lambda_2^B)Z^2Z_\Delta^2\Delta_{ab}\Delta_{ba}$ into Φ_1. The Φ_1 terms correspond to the Hartree-Fock approximation and agree with the remaining terms of Eq. (4.4) of [9]. The remaining $\mathcal{O}(\hbar^2)$ terms in $\Gamma_3^{(3)}$ give the sunset diagrams on replacing $\bar{V}$ and V_N by the solution of their equations of motion at $\mathcal{O}(\hbar^0)$, which give $V_N = 3\bar{V} = -Z_V^{-1}(\lambda+\delta\lambda)v\times\delta^{(4)}(x-y)\delta^{(4)}(x-z)$. We find that Z_V cancels on elimination of $\bar{V}$ and V_N. It also disappears from the Ward identity once $\bar{V}$ is eliminated and, hence, plays no role in the further development.

Going to momentum space, the final result is (up to an irrelevant constant)

$$\Gamma^{(3)} = \int_x\left(-Z_\Delta^{-1}\frac{m^2+\delta m_0^2}{2}v^2 - \frac{\lambda+\delta\lambda_0}{4!}v^4\right) + \frac{i\hbar}{2}(N-1)\mathrm{Tr}\ln(\Delta_G^{-1}) + \frac{i\hbar}{2}\mathrm{Tr}\ln(\Delta_H^{-1})$$
$$-\frac{i\hbar}{2}(N-1)\int_k\left(-ZZ_\Delta k^2 + m^2 + \delta m_1^2 + Z_\Delta\frac{\lambda+\delta\lambda_1^A}{6}v^2\right)\Delta_G(k)$$
$$-\frac{i\hbar}{2}\int_k\left(-ZZ_\Delta k^2 + m^2 + \delta m_1^2 + Z_\Delta\frac{3\lambda+\delta\lambda_1^A+2\delta\lambda_1^B}{6}v^2\right)\Delta_H(k)$$
$$+\frac{\hbar^2}{24}[(N+1)\lambda + (N-1)\delta\lambda_2^A + 2\delta\lambda_2^B]Z_\Delta^2(N-1)\int_k\Delta_G(k)\Delta_G(k)$$
$$+\frac{\hbar^2}{24}[3\lambda+\delta\lambda_2^A+2\delta\lambda_2^B]Z_\Delta^2\int_k\Delta_H(k)\Delta_H(k) + \frac{\hbar^2}{24}2(\lambda+\delta\lambda_2^A)Z_\Delta^2(N-1)\int_k\Delta_G(k)\Delta_H(k)$$
$$+\frac{\hbar^2}{4}\left[\frac{(\lambda+\delta\lambda)v}{3}\right]^2Z_\Delta^3(N-1)\int_{kl}\Delta_H(k)\Delta_G(l)\Delta_G(k+l)$$
$$+\frac{\hbar^2}{12}[(\lambda+\delta\lambda)v]^2Z_\Delta^3\int_{kl}\Delta_H(k)\Delta_H(l)\Delta_H(k+l). \tag{B5}$$

From this expression, we derive the renormalized equations of motion (4.14)–(4.16)

The divergent integrals $\mathcal{T}_{G/H}$ (4.17) and $\mathcal{I}_{HG}(p)$ (4.18) enter into the equations of motion. $\mathcal{I}_{HG}(p)$ can be rendered finite by a single subtraction,

$$\mathcal{I}_{HG}(p) = \mathcal{I}^{\mu} + \mathcal{I}^{\rm fin}_{HG}(p), \tag{B6}$$

where $\mathcal{I}^{\mu} = \int_q [i\Delta^{\mu}(q)]^2$. Since we wrote the propagators with the physical masses explicit, it is crucial to also subtract a portion of the finite piece $\mathcal{I}^{\rm fin}_{HG}(m_{G/H})$ so that the pole of the propagator is fixed at the physical mass of the Goldstone/Higgs propagator, respectively. We make this subtraction separately so as to have a universal $\mathcal{I}^{\mu}$.

The tadpole integrals $\mathcal{T}_{G/H}$ require two subtractions each since $\int_q i[\Delta^{\mu}(q)]^2\Sigma^0_{G/H}(q)$ is logarithmically divergent. To that end we introduce

$$\Sigma^{\mu}(q) = -i\hbar\left[\frac{(\lambda+\delta\lambda)v}{3}\right]^2 Z_{\Delta}^3 \times\left[\int_{\ell} i\Delta^{\mu}(\ell) i\Delta^{\mu}(q+\ell) - \mathcal{I}^{\mu}\right], \tag{B7}$$

which is asymptotically the same as $\Sigma^0_{G/H}(q)$, so that $\int_q i[\Delta^{\mu}(q)]^2[\Sigma^0_{G/H}(q) - \Sigma^{\mu}(q)]$ is finite. For later convenience we write

$$\int_q i[\Delta^{\mu}(q)]^2\Sigma^{\mu}(q) = \hbar\left[\frac{(\lambda+\delta\lambda)v}{3}\right]^2 Z_{\Delta}^3 c^{\mu}. \tag{B8}$$

Then

$$\mathcal{T}_{G/H} = \mathcal{T}^{\mu} - i(m^2_{G/H} - \mu^2)\mathcal{I}^{\mu} + \hbar\left[\frac{(\lambda+\delta\lambda)v}{3}\right]^2 Z_{\Delta}^3 c^{\mu} + \mathcal{T}^{\rm fin}_{G/H}, \tag{B9}$$

where $\mathcal{T}^{\mu} = \int_q i\Delta^{\mu}(q)$. Note that $\mathcal{T}^{\mu}$ and c^{μ} are real and $\mathcal{I}^{\mu}$ is imaginary, so that all of the subtractions can be absorbed into real counterterms.

The counterterms are found by eliminating $m^2_{G/H}$ and demanding that the divergences proportional to different powers of v^2 and $\mathcal{T}^{\rm fin}_{G/H}$ separately vanish. Further, we enforce $\Delta_G^{-1}(m_G) = 0$ and $\Delta_H^{-1}(m_H) = 0$ and that the counterterms are momentum independent. This gives eight equations for the seven constants $Z, Z_{\Delta}, \delta m_1^2, \delta\lambda_1^A, \delta\lambda_2^A, \delta\lambda_2^B$ and $\delta\lambda$, however one of them is redundant and a solution exists [19].

We find nontrivial field strength renormalizations,

$$Z = Z_{\Delta}^{-1} = \left\{1 + \frac{i\hbar\lambda}{3}[\mathcal{I}^{\rm fin}_{HG}(m_H) - \mathcal{I}^{\rm fin}_{HG}(m_G)]\right\}^2, \tag{B10}$$

and a nonzero

$$\delta\lambda = -\lambda \pm \lambda\left\{1 + \frac{i\hbar\lambda}{3}[\mathcal{I}^{\rm fin}_{HG}(m_H) - \mathcal{I}^{\rm fin}_{HG}(m_G)]\right\}^3 \tag{B11}$$

(the two solutions arise because $\delta\lambda$ only enters the equations of motion in the quadratic combination $(\lambda+\delta\lambda)^2$). These counterterms are normally trivial ($Z = Z_{\Delta} = 1$ and $\delta\lambda = 0$) for ϕ^4 theory at two loops. However, due to the modification of the Higgs equation of motion, we require $Z_{\Delta} \neq 1$ in order to enforce $\Delta_H^{-1}(m_H) = 0$ and this is then compensated by Z and $\delta\lambda$ in order to recover the other renormalization conditions. The other counterterms can be obtained for any regulator, but the expressions are bulky and unenlightening even for dimensional regularization in $d = 4 - 2\epsilon$ dimensions, so we leave their explicit forms in the supplemental Mathematica notebook.

APPENDIX C: AUXILIARY VERTEX AND RENORMALIZATION IN THREE AND FOUR DIMENSIONS

As described in Sec. IV B the renormalization of the three-loop 3PIEA requires the definition of an auxiliary vertex V^{μ}_{abc} with the same asymptotic behavior as the full self-consistent solution at large momentum. This auxiliary vertex can be found in terms of a six-point kernel which obeys the integral equation (4.29) illustrated in Fig. 6. Solving (4.29) by iteration generates an infinite number of terms, one of which is illustrated in Fig. 14. Each contribution is in one-to-one correspondence with the sequence of permutations $\pi_1\pi_2\cdots\pi_n\cdots$ of the propagator lines (read from left to right in relation to the diagram). Now we divide the permutations into two classes: "stabilizers," for which $\pi(a) = a$, and "derangements," for which $\pi(a) = b$ or c.

Any sequence of permutations is of the form of an alternating sequence of runs of (possibly zero) stabilizers, separated by derangements. Consider a run of n stabilizers, $\cdots\pi_a(\pi_1\pi_2\cdots\pi_n)\pi_b\cdots$, where π_a and π_b are derangements and π_1 through π_n are all stabilizers. The case for $n = 2$ is shown in Fig. 14. Each stabilizer creates a logarithmically divergent loop on the bottom two lines $\sim -\lambda\mathcal{I}^{\mu}$. Derangements on the other hand, if they create loops at all, create loops with > 2 propagators, and hence are convergent. Thus all divergences in $\mathcal{K}_{abcdef}$ can be removed by rendering a single primitive divergence finite. Note that the whole series $\sum_{n=0}^{\infty}\cdots\pi_a(\prod_{i=1}^{n}\pi_i)\pi_b$, where again $\pi_{a,b}$ are derangements and $\{\pi_i\}$ are stabilizers, can be summed because the series is geometric. The result is that the six-point kernel can be determined by an equation like

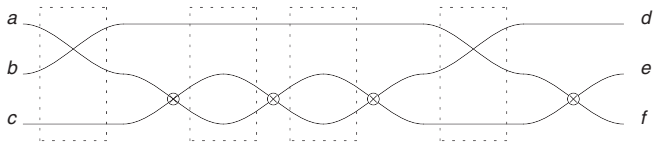

FIG. 14. A contribution to the six-point kernel $\mathcal{K}_{abcdef}$ resulting from (left to right) a derangement, two stabilizers and another derangement. The dashed boxes surround the permutations (to aid visualization only). Only stabilizers lead to divergent loops.

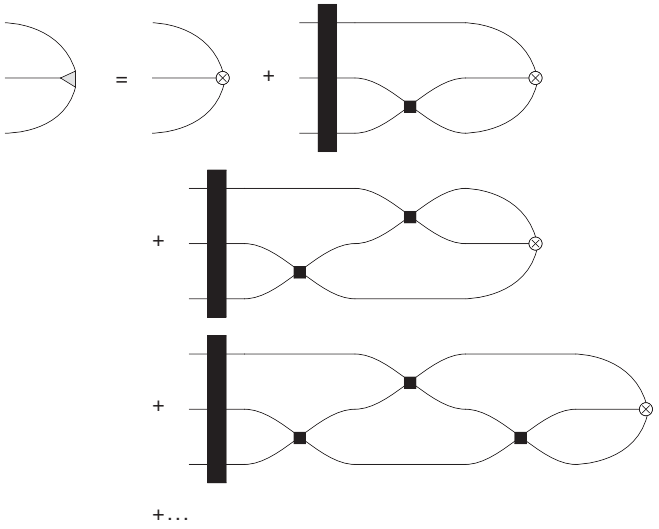

FIG. 15. Solution for the auxiliary vertex V^{μ}_{abc} in terms of the four-point kernel which sums all iterated bubble insertions.

(4.29), except that the sum over all permutations is replaced by a sum over derangements only, and the bare vertex W is replaced by a four-point kernel $\mathcal{K}^{(4)}_{abcd} \sim \lambda/(1+\lambda\mathcal{I}^{\mu})$. Denoting this four-point kernel by a square vertex, we can finally write the solution for V^{μ}_{abc} in Fig. 15.

This expression for V^{μ}_{abc} can be dramatically simplified in 3 or $1+2$ dimensions because $\mathcal{I}^{\mu}$ is finite and the geometric sum in $\mathcal{K}_{abcd}$ converges. Indeed $\mathcal{K}^{(4)}_{abcd}(p_1,p_2,p_3,p_1+p_2-p_3) \sim \lambda/[1+\lambda/(p_1+p_2)^{4-d}] \to \lambda$ as $p_{1,2,3,4} \to \infty$. Further, every loop integral in Fig. 15 likewise converges, and every loop yields a factor of $\sim 1/p^{4-d}$. Thus, the dominant behavior as $p \to \infty$ is just the tree-level behavior and we can eliminate the auxiliary vertex completely.

However, in 4 or $1+3$ dimensions V^{μ}_{abc} apparently cannot be simplified further. First $\mathcal{K}^{(4)}_{abcd}$ must be renormalized, then the bubble appearing in the nontrivial terms in Fig. 15 (or the equivalent integral equation) must be renormalized, then the resulting series must be summed (or the equivalent integral equation solved), noting that on the basis of power counting every term is apparently equally important. On this basis we expect that no compact analytic expression for V^{μ}_{abc}, or even its asymptotic behavior, exists and that the renormalization must be accomplished as part of the self-consistent numerical solution of the full equations of motion.

This style of argument can be quickly generalized to many other theories, such as gauge theories, where the diagrammatic expansion has a similar combinatorial structure to scalar $O(N)$ theory, showing up the well known problem of the renormalization of nPIEA for $n \geq 3$ in four dimensions. The discussion here certainly does not solve this problem, which remains open, to our knowledge, though we hope this discussion may be helpful.

APPENDIX D: DERIVING COUNTERTERMS FOR THREE-LOOP TRUNCATIONS

In this section we work in $1+2$ dimensions as discussed in Sec. IV B. The effective action is as in Appendix B (before eliminating $\bar{V}$ and V_N) except we introduce a new counterterm $\delta\lambda \to \delta\lambda_C$ for the second term in (B2) and add the three-loop diagrams,

$$\Phi_3 = Z_V^4 Z_\Delta^6 \left[(N-1)\frac{i\hbar^3}{3!} V_N (\bar{V})^3 (\Delta_H)^3 (\Delta_G)^3 + \frac{i\hbar^3}{4!}(V_N)^4 (\Delta_H)^6 + (N-1)\frac{i\hbar^3}{8}(\bar{V})^4 \Delta_H \Delta_H (\Delta_G)^4 \right], \tag{D1}$$

$$\Phi_4 = \frac{i\hbar^3(\lambda+\delta\lambda)}{24} Z_V^2 Z_\Delta^5 [2(N-1)\bar{V} V_N (\Delta_H)^3 \Delta_G \Delta_G + (N^2-1)\bar{V}\,\bar{V}\,\Delta_H (\Delta_G)^4 + 3 V_N V_N (\Delta_H)^5 + 2^2 (N-1)\bar{V}\,\bar{V}\,(\Delta_G)^3 \Delta_H \Delta_H], \tag{D2}$$

$$\Phi_5 = \frac{i\hbar^3(\lambda+\delta\lambda)^2}{144} Z_\Delta^4 \{ [(N-1)\Delta_G \Delta_G + \Delta_H \Delta_H]^2 + 2(N-1)(\Delta_G)^4 + 2(\Delta_H)^4 \}. \tag{D3}$$

The equations of motion following from $\Gamma^{(3)}$ are then

$$\begin{aligned}
\Delta_G^{-1} = &-\left(Z Z_\Delta \partial_\mu \partial^\mu + m^2 + \delta m_1^2 + Z_\Delta \frac{\lambda + \delta\lambda_1^A}{6} v^2 \right) \\
&- \frac{\hbar}{6}[(N+1)\lambda + (N-1)\delta\lambda_2^A + 2\delta\lambda_2^B] Z_\Delta^2 \mathcal{T}_G - \frac{\hbar}{6}(\lambda + \delta\lambda_2^A) Z_\Delta^2 \mathcal{T}_H - i\hbar Z_V^2 Z_\Delta^3 \left[-2\frac{(\lambda+\delta\lambda_C) Z_V^{-1} v}{3} - \bar{V} \right] \Delta_H \Delta_G \bar{V} \\
&+ \hbar^2 Z_V^4 Z_\Delta^6 [V_N (\bar{V})^3 (\Delta_H)^3 (\Delta_G)^2 + (\bar{V})^4 \Delta_H \Delta_H (\Delta_G)^3] \\
&+ \frac{\hbar^2(\lambda+\delta\lambda)}{3} Z_V^2 Z_\Delta^5 [\bar{V} V_N (\Delta_H)^3 \Delta_G + (N+1)\bar{V}\,\bar{V}\,\Delta_H (\Delta_G)^3 + 3\bar{V}\,\bar{V}\,(\Delta_G)^2 \Delta_H \Delta_H] \\
&+ \frac{\hbar^2(\lambda+\delta\lambda)^2}{18} Z_\Delta^4 [(N+1)(\Delta_G)^3 + \Delta_H \Delta_H \Delta_G],
\end{aligned} \tag{D4}$$

for the Goldstone propagator,

$$\bar{V} = -\frac{(\lambda+\delta\lambda_C)v}{3} Z_V^{-1} + i\hbar Z_V^2 Z_\Delta^3 [V_N(\bar{V})^2(\Delta_H)^2\Delta_G + (\bar{V})^3\Delta_H(\Delta_G)^2] + \frac{i\hbar(\lambda+\delta\lambda)}{6} Z_\Delta^2 [V_N(\Delta_H)^2 + (N+1)\bar{V}(\Delta_G)^2 + 4\bar{V}\Delta_G\Delta_H], \tag{D5}$$

for the Higgs-Goldstone-Goldstone vertex,

$$V_N = -(\lambda+\delta\lambda_C)vZ_V^{-1} + i\hbar Z_V^2 Z_\Delta^3 [(N-1)(\bar{V})^3(\Delta_G)^3 + (V_N)^3(\Delta_H)^3] + \frac{i\hbar(\lambda+\delta\lambda)}{2} Z_\Delta^2 [(N-1)\bar{V}\Delta_G\Delta_G + 3V_N(\Delta_H)^2], \tag{D6}$$

for the triple Higgs vertex, and finally

$$0 = \Delta_G^{-1}(p=0)v, \tag{D7}$$

$$0 = Z_V Z_\Delta \bar{V}(p,-p,0)v + \Delta_G^{-1}(p) - \Delta_H^{-1}(p), \tag{D8}$$

for the Ward identities.

Note that the only divergent integrals in these equations are the linearly divergent tadpole integrals $\mathcal{T}_{G/H}$ and the logarithmically divergent BBALL integrals [last line of (D4)]. By power counting with reference to Fig. 7, one finds that the third, fourth, and fifth lines of (D4) produce finite self-energy contributions with leading asymptotics $\sim p^{-1}$, p^{-4}, and p^{-2}, respectively. We can separate finite and divergent parts of Δ_G^{-1} as

$$\Delta_G^{-1} = -\left(\partial_\mu\partial^\mu + m^2 + \frac{\lambda}{6}v^2\right) - [\Sigma_G^0(p) - \Sigma_G^0(m_G)] - \Sigma_G^\infty(p), \tag{D9}$$

where

$$\begin{aligned} -\Sigma_G^0(p) = {} & -\frac{\hbar}{6}(N+1)\lambda(\mathcal{T}_G - \mathcal{T}^\mu) - \frac{\hbar}{6}\lambda(\mathcal{T}_H - \mathcal{T}^\mu) \\ & - i\hbar\left[-2\frac{(\lambda+\delta\lambda_C)Z_V^{-1}v}{3} - \bar{V}\right]\Delta_H\Delta_G\bar{V} + \hbar^2[V_N(\bar{V})^3(\Delta_H)^3(\Delta_G)^2 + (\bar{V})^4\Delta_H\Delta_H(\Delta_G)^3] \\ & + \frac{\hbar^2(\lambda+\delta\lambda)Z_\Delta^2}{3}[\bar{V}V_N(\Delta_H)^3\Delta_G + (N+1)\bar{V}\,\bar{V}\,\Delta_H(\Delta_G)^3 + 3\bar{V}\,\bar{V}\,(\Delta_G)^2\Delta_H\Delta_H] \\ & + \frac{\hbar^2(\lambda+\delta\lambda)^2 Z_\Delta^4}{18}[(N+1)(\Delta_G)^3 + \Delta_H\Delta_H\Delta_G - (N+2)\mathcal{B}^\mu], \end{aligned} \tag{D10}$$

and

$$\begin{aligned} -\Sigma_G^\infty(p) = {} & -\Sigma_G^0(m_G) - \left((ZZ_\Delta - 1)\partial_\mu\partial^\mu + \delta m_1^2 + \frac{\delta\lambda_1^A}{6}v^2 + (Z_\Delta - 1)\frac{\lambda+\delta\lambda_1^A}{6}v^2\right) \\ & - \frac{\hbar}{6}(N+1)\lambda\mathcal{T}^\mu - \frac{\hbar}{6}[(N-1)\delta\lambda_2^A + 2\delta\lambda_2^B]\mathcal{T}_G - \frac{\hbar}{6}[(N+1)\lambda + (N-1)\delta\lambda_2^A + 2\delta\lambda_2^B](Z_\Delta^2 - 1)\mathcal{T}_G \\ & - \frac{\hbar}{6}\lambda\mathcal{T}^\mu - \frac{\hbar}{6}\delta\lambda_2^A\mathcal{T}_H - \frac{\hbar}{6}(\lambda+\delta\lambda_2^A)(Z_\Delta^2 - 1)\mathcal{T}_H \\ & - i\hbar(Z_V^2 Z_\Delta^3 - 1)\left[-2\frac{(\lambda+\delta\lambda_C)Z_V^{-1}v}{3} - \bar{V}\right]\Delta_H\Delta_G\bar{V} \\ & + \hbar^2(Z_V^4 Z_\Delta^6 - 1)[V_N(\bar{V})^3(\Delta_H)^3(\Delta_G)^2 + (\bar{V})^4\Delta_H\Delta_H(\Delta_G)^3] \\ & + \frac{\hbar^2(\lambda+\delta\lambda)Z_\Delta^2}{3}(Z_V^2 Z_\Delta^3 - 1)[\bar{V}V_N(\Delta_H)^3\Delta_G + (N+1)\bar{V}\,\bar{V}\,\Delta_H(\Delta_G)^3 + 3\bar{V}\,\bar{V}\,(\Delta_G)^2\Delta_H\Delta_H] \\ & + (N+2)\frac{\hbar^2(\lambda+\delta\lambda)^2 Z_\Delta^4}{18}\mathcal{B}^\mu, \end{aligned} \tag{D11}$$

are the finite and divergent parts, respectively, and we introduced the BBALL integral $\mathcal{B}^\mu = \int_{qp} \Delta^\mu(q)\Delta^\mu(p)\Delta^\mu(p+q)$. In this split we have already assumed that $(\lambda+\delta\lambda_C)Z_V^{-1}$ and $(\lambda+\delta\lambda)Z_\Delta^2$ are finite, which will turn out to be the case. Renormalization requires $\Sigma_G^\infty(p)=0$. Note the explicit subtraction of $\Sigma_G^0(m_G)$ in order to fulfill the mass shell condition. Doing the same now for Δ_H^{-1}, we find the pole condition

$$0 = Z_V Z_\Delta \bar{V}(m_H,-m_H,0)v + m_H^2 - m_G^2 - \Sigma_G^0(m_H), \tag{D12}$$

which requires

$$Z_V Z_\Delta = \frac{m_G^2 + \Sigma_G^0(m_H) - m_H^2}{\bar{V}(m_H,-m_H,0)v} \equiv \kappa, \tag{D13}$$

which is finite. We take for our other renormalization conditions the separate vanishing of kinematically independent divergences, implying

$$ZZ_\Delta = 1, \tag{D14}$$

$$\delta m_1^2 = -\Sigma_G^0(m_G) - \frac{\hbar}{6}(N+2)\lambda\mathcal{T}^\mu + (N+2)\frac{\hbar^2\lambda^2}{18}\mathcal{B}^\mu, \tag{D15}$$

$$\delta\lambda_1^A = -\frac{(Z_\Delta-1)\lambda}{Z_\Delta} \tag{D16}$$

$$Z_V^2 Z_\Delta^3 = 1, \tag{D17}$$

$$0 = (N-1)\delta\lambda_2^A + 2\delta\lambda_2^B + [(N+1)\lambda + (N-1)\delta\lambda_2^A + 2\delta\lambda_2^B](Z_\Delta^2-1), \tag{D18}$$

$$0 = \delta\lambda_2^A + (\lambda+\delta\lambda_2^A)(Z_\Delta^2-1). \tag{D19}$$

We also choose the conditions

$$(\lambda+\delta\lambda)Z_\Delta^2 = \lambda, \tag{D20}$$

$$(\lambda+\delta\lambda_C)Z_V^{-1} = \lambda, \tag{D21}$$

to recover the tree-level asymptotics for $\bar{V}$ and V_N. These conditions give a closed system of nine equations for the nine quantities Z, Z_Δ, Z_V, δm_1^2, $\delta\lambda_1^A$, $\delta\lambda_2^{A/B}$, $\delta\lambda$, and $\delta\lambda_C$.

These conditions determine

$$\delta\lambda_2^A = \delta\lambda_2^B = -\frac{\lambda(Z_\Delta^2-1)}{Z_\Delta^2} = (\kappa^2-1)\lambda, \tag{D22}$$

$$Z_V = \kappa^3, \tag{D23}$$

$$Z_\Delta = \kappa^{-2}, \tag{D24}$$

$$Z = \kappa^2, \tag{D25}$$

$$\delta\lambda = (\kappa^4-1)\lambda, \tag{D26}$$

$$\delta\lambda_C = (\kappa^3-1)\lambda. \tag{D27}$$

Note that if $\kappa = 1$ all of the counterterms except δm_1^2 vanish. This is a manifestation of the super-renormalizability of ϕ^4 theory in $1+2$ dimensions. The nonzero, indeed finite, values of all of the other counterterms are not required to UV-renormalize the theory, but only to maintain the pole condition for the Higgs propagator despite the vertex Ward identity.

[1] There is a vast literature. For a pedagogical review, see e.g. Henriette Elvang and Yu-tin Huang, Scattering Amplitudes, arXiv:1308.1697 and for an implementation, see e.g. C. F. Berger, Z. Bern, L. J. Dixon, F. F. Cordero, D. Forde, H. Ita, D. A. Kosower, and D. Maître, Automated implementation of on-shell methods for one-loop amplitudes, Phys. Rev. D **78**, 036003 (2008).

[2] J. Berges, Introduction to nonequilibrium quantum field theory, AIP Conf. Proc. **739**, 3 (2004).

[3] M. E. Carrington, The 4PI effective action for ϕ^4 theory, Eur. Phys. J. C **35**, 383 (2004).

[4] M. E. Carrington and Y. Guo, Techniques for n-particle irreducible effective theories, Phys. Rev. D **83**, 016006 (2011).

[5] M. E. Carrington and Y. Guo, New method to calculate the n-particle irreducible effective action, Phys. Rev. D **85**, 076008 (2012).

[6] See e.g. A. Cherman, D. Dorigoni, G. V. Dunne, and M. Ünsal, Resurgence in Quantum Field Theory: Nonperturbative Effects in the Principal Chiral Model, Phys. Rev. Lett. **112**, 021601 (2014); D. Dorigoni, An Introduction to Resurgence, Trans-Series and Alien Calculus, arXiv:1411.3585.

[7] M. C. Abraao York and G. D. Moore, 2PI Resummation in 3D SU(N) Higgs Theory, J. High Energy Phys. 10 (2014) 105.

[8] Mark C. A. York, G. D. Moore, and M. Tassler, 3-loop 3PI effective action for 3D SU(3) QCD, J. High Energy Phys. 06 (2012) 077.

[9] A. Pilaftsis and D. Teresi, Symmetry-improved CJT effective action, Nucl. Phys. **B874**, 594 (2013).
[10] See e.g. H. V. Hees and J. Knoll, Renormalization in self-consistent approximation schemes at finite temperature. III. Global symmetries, Phys. Rev. D **66**, 025028 (2002); J. Berges, Sz Borsányi, U. Reinosa, and J. Serreau, Non-perturbative renormalization for 2PI effective action techniques, Ann. Phys. (N.Y.) **320**, 344 (2005); M. E. Carrington and E. Kovalchuk, Leading order QCD shear viscosity from the three-particle irreducible effective action, Phys. Rev. D **80**, 085013 (2009).
[11] John M. Cornwall, R. Jackiw, and E. Tomboulis, Effective action for composite operators, Phys. Rev. D **10**, 2428 (1974).
[12] J. Smolic and M. Smolic, 2PI effective action and evolution equations of $N = 4$ super Yang-Mills, Eur. Phys. J. C **72**, 2106 (2012).
[13] M. Garny and M. M. Müller, Kadanoff-Baym equations with non-Gaussian initial conditions: The equilibrium limit, Phys. Rev. D **80**, 085011 (2009); R. Van Leeuwen and G. Stefanucci, Wick theorem for general initial states, Phys. Rev. B **85**, 115119 (2012); Robert van Leeuwen and G. Stefanucci, Equilibrium and nonequilibrium many-body perturbation theory: A unified framework based on the Martin-Schwinger hierarchy, J. Phys. Conf. Ser. **427**, 012001 (2013).
[14] J. I. Kapusta and C. Gale, *Finite-Temperature Field Theory: Principles and Applications* (Cambridge University Press, Cambridge, England, 2006).
[15] J. Rammer and H. Smith, Quantum field-theoretical methods in transport theory of metals, Rev. Mod. Phys. **58**, 323 (1986); G. Stefanucci and Robert van Leeuwen, *Nonequilibrium Many-Body Theory of Quantum Systems* (Cambridge University Press, Cambridge, England, 2013).
[16] J. Goldstone, A. Salam, and S. Weinberg, Broken symmetries, Phys. Rev. **127**, 965 (1962); G. Jona-Lasinio, Relativistic field theories with symmetry-breaking solutions, Nuovo Cimento **34**, 1790 (1964).
[17] J Zinn-Justin, *Quantum Field Theory and Critical Phenomena*, 1st ed. (Oxford University Press, New York, 1990).
[18] J. Berges, N-particle irreducible effective action techniques for gauge theories, Phys. Rev. D **70**, 105010 (2004).
[19] See Supplemental Material at http://link.aps.org/supplemental/10.1103/PhysRevD.91.085020 for MATHEMATICA notebooks which verify tensor manipulations and compute counter-terms.
[20] G. Fejos, A. Patkós, and Zs Szép, Renormalisability of the 2PI-Hartree approximation of multicomponent scalar models in the broken symmetry phase, Nucl. Phys. **A803**, 115 (2008); A. Patkós and Zs Szép, Non-perturbative construction of counterterms for 2PI-approximation, Nucl. Phys. **A820**, 255c (2009).
[21] G. Markó, U. Reinosa, and Z. Szép, Broken phase effective potential in the two-loop Φ-derivable approximation and nature of the phase transition in a scalar theory, Phys. Rev. D **86**, 085031 (2012).
[22] A. Patkós and Zs Szép, Counterterm resummation for 2PI-approximation in constant background, Nucl. Phys. **A811**, 329 (2008).
[23] S. Weinberg, High-energy behavior in quantum field theory, Phys. Rev. **118**, 838 (1960).
[24] H. Mao, On the symmetry improved CJT formalism in the O(4) linear sigma model, Nucl. Phys. **A925**, 185 (2014).
[25] N. Petropoulos, Linear sigma model at finite temperature, arXiv:hep-ph/0402136.
[26] E. Jones and T. Oliphant and P. Peterson, others, SciPy: Open source scientific tools for Python, http://www.scipy.org/.
[27] S. Coleman, There are no Goldstone bosons in two dimensions, Commun. Math. Phys. **31**, 259 (1973).
[28] M. Shifman, *Advanced Topics in Quantum Field Theory: A Lecture Course* (Cambridge University Press, Cambridge, England, 2012).
[29] M. E. Peskin and D. V. Schroeder, *An Introduction to Quantum Field Theory* (Westview Press, Boulder, Colorado, 1995).
[30] S. Weinberg, *The Quantum Theory of Fields, Volume 1: Foundations* (Cambridge University Press, Cambridge, England, 2005).
[31] A. Pilaftsis and D. Teresi, Symmetry improved 2PI effective action and the infrared divergences of the standard model, arXiv:1502.07986.
[32] M. E. Carrington, Wei-jie Fu, D. Pickering, and J. W. Pulver, Renormalization group methods and the 2PI effective action, Phys. Rev. D **91**, 025003 (2015).